Magnetism beyond the 3d transition metal oxides

Priya Mahadevan

Department of Condensed Matter Physics & Material Science

S.N.Bose National Centre for Basic Sciences

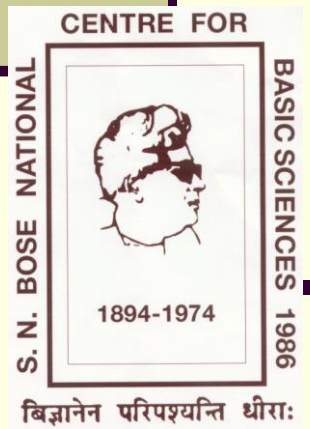

ICTS, May 2017

Where do we expect magnetism ?

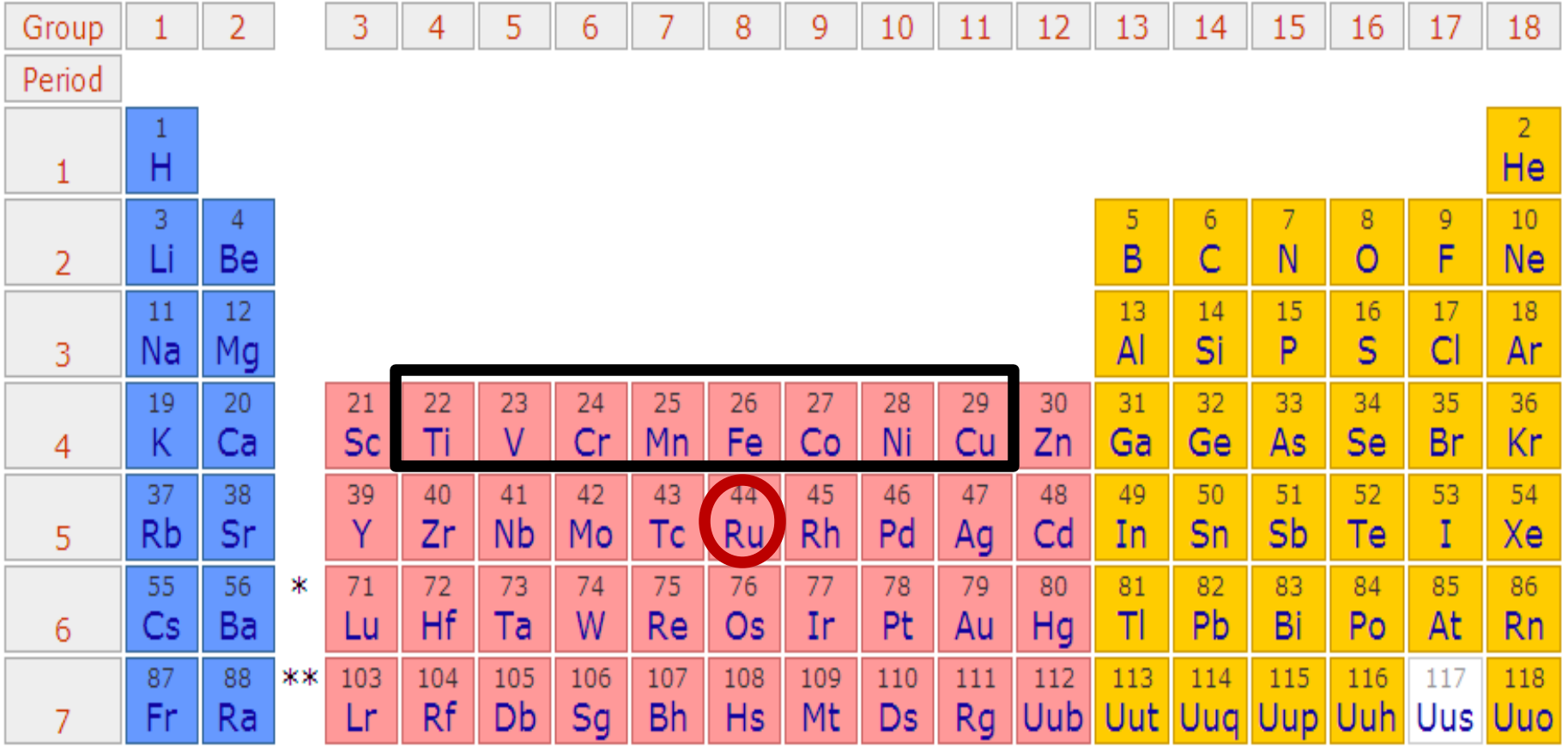

Why do we expect magnetism there?

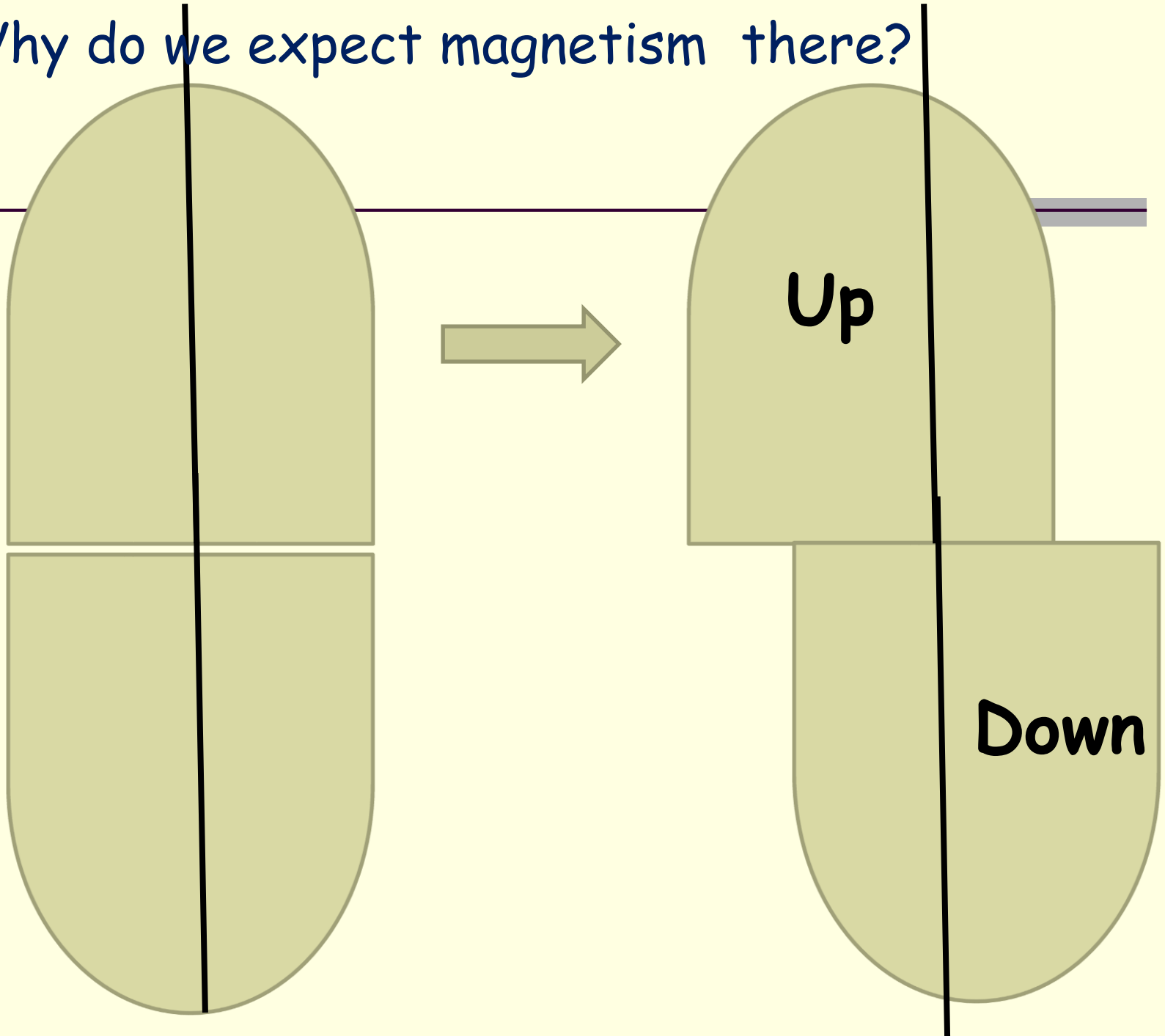

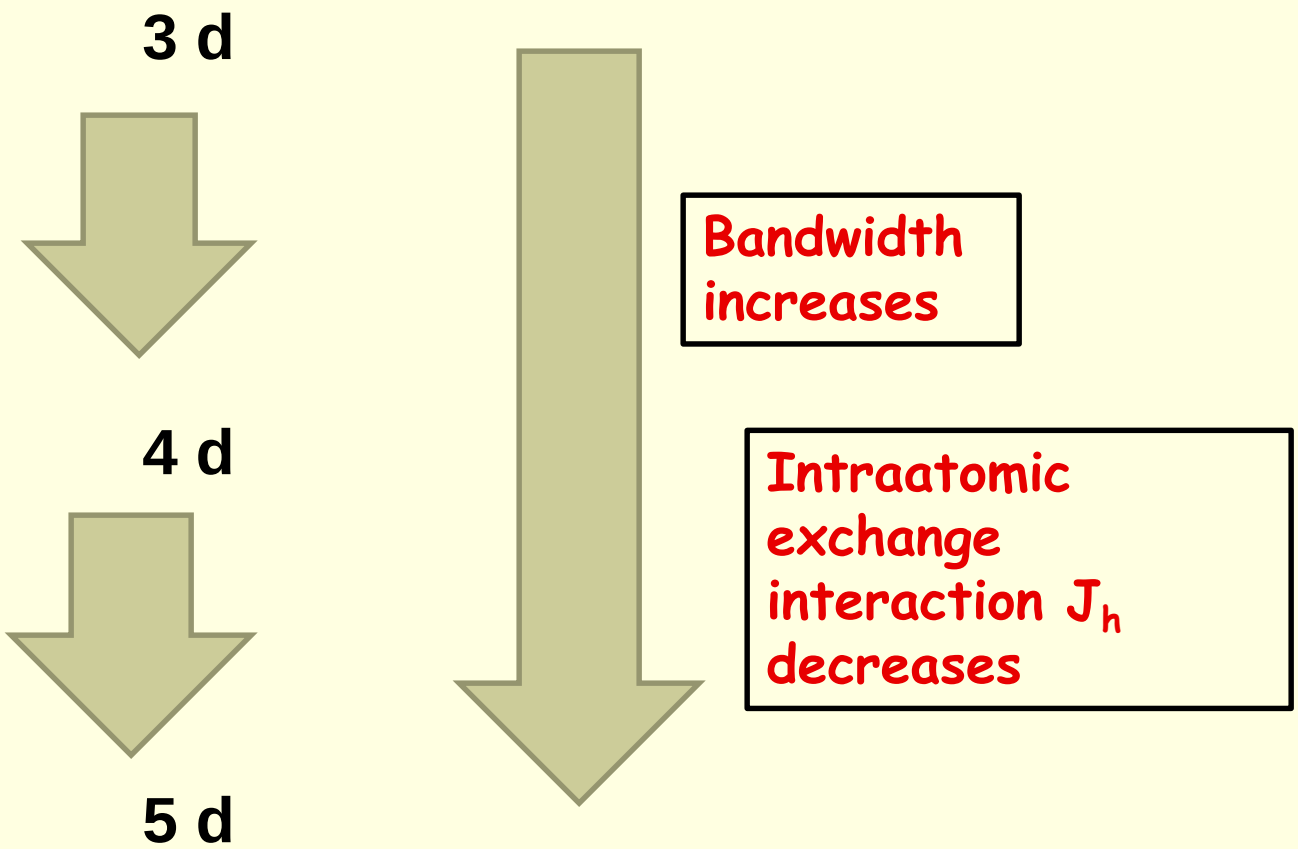
3 d
4 d
5 d
Bandwidth increases
Intraatomic exchange interaction J_h decreases

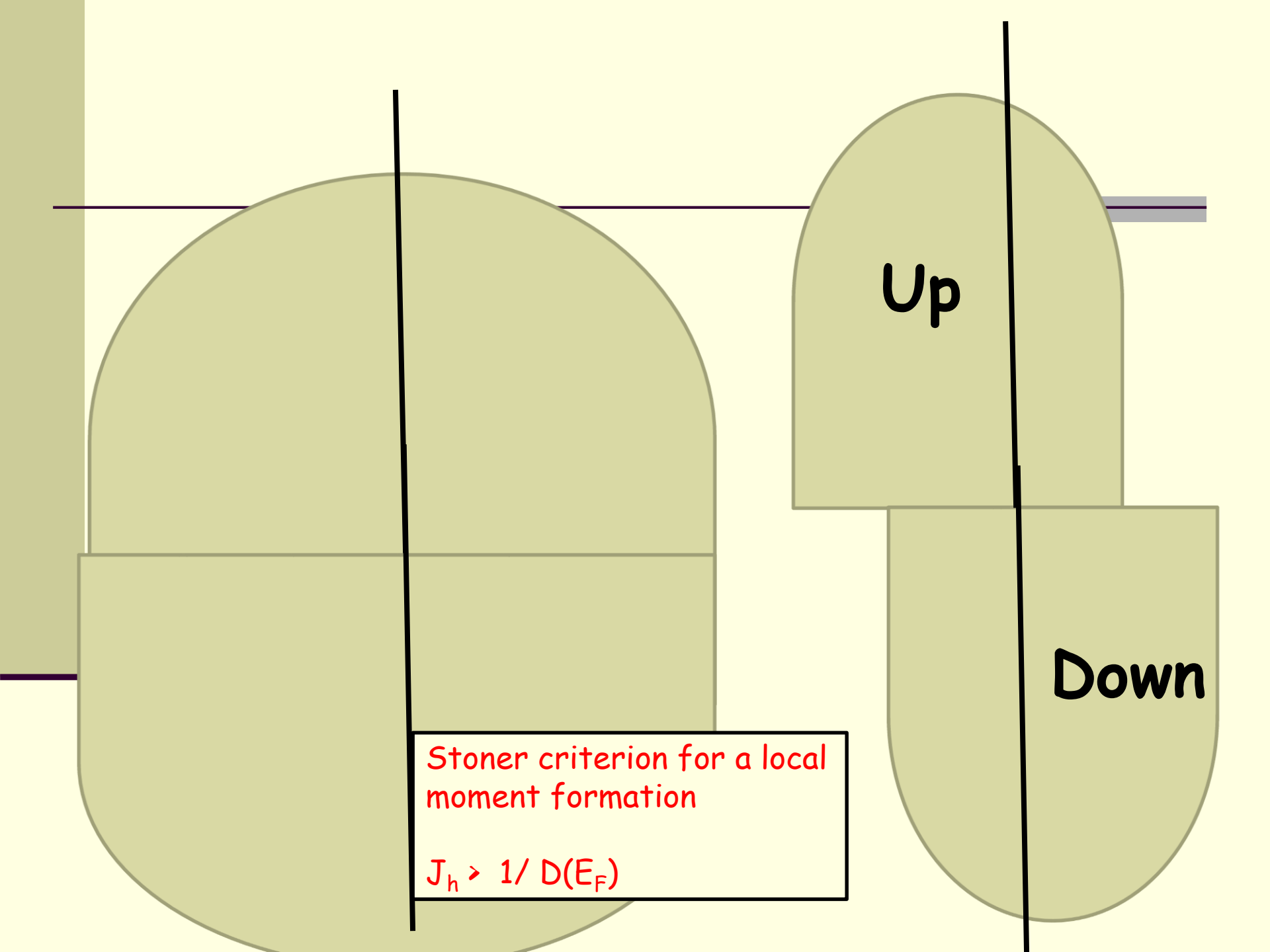
Up
Down
Stoner criterion for a local moment formation
$J_h > 1/ D(E_F)$

A moment is difficult to sustain in a 4d/5d oxide,

A high magnetic ordering temperature is not expected

SrMnO3	233 K	(PRB 64, 134412 (2011).
SrTcO3	1023 K	(PRL 106, 067201 (2011).
CaTcO3	800 K	(JACS 133, 1654 (2011).

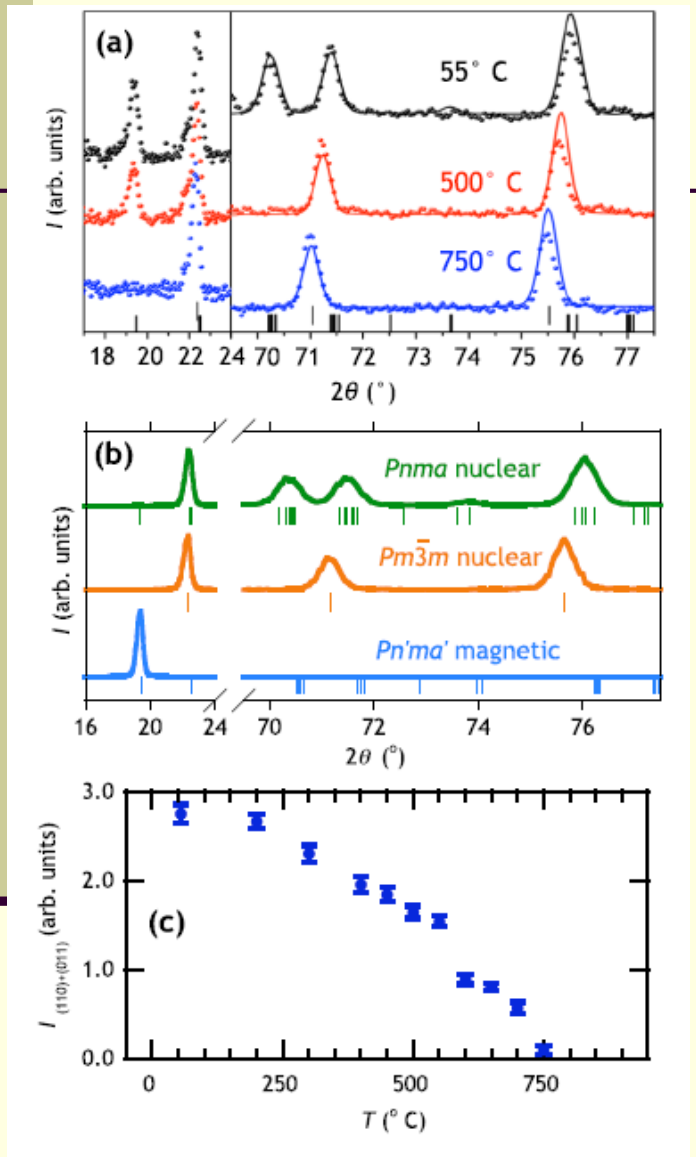

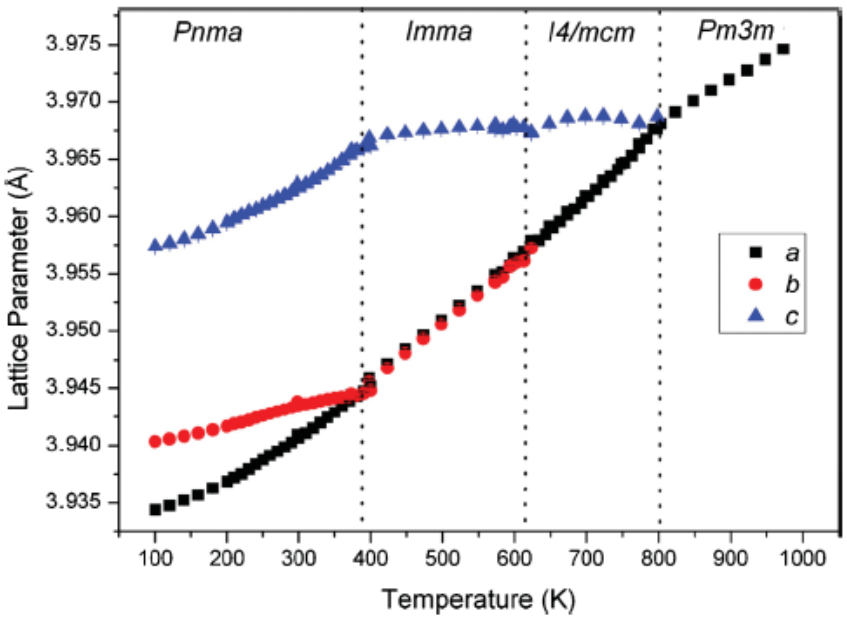

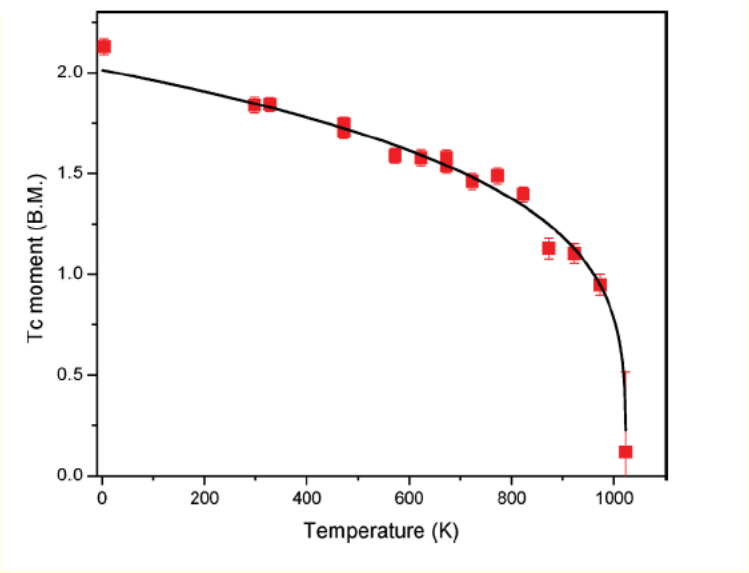

Rodriguez et al., PRL 106, 067201 (2011); Thorgood et al., Dalton Trans, 40, 7228 (2011).

Could distortions be the origin for the enhancement?

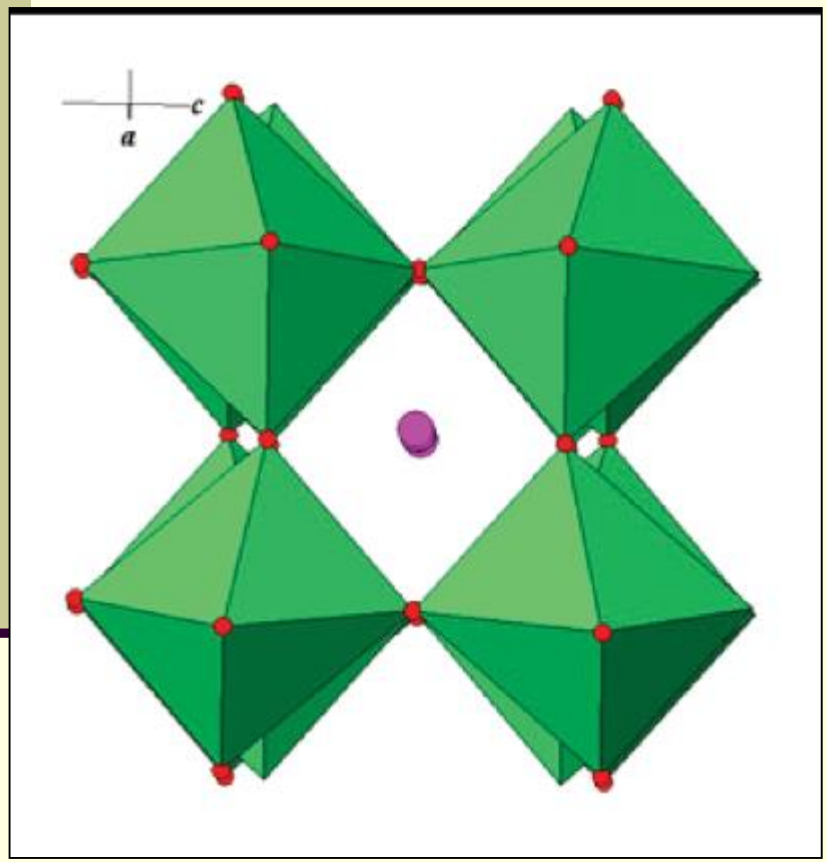

$GdFeO_3$ distortions

Tc-O-Tc angle in $CaTcO_3$ is 150-152

Mn-O-Mn angle in $SrMnO_3$ is 180

$SrTcO_3$

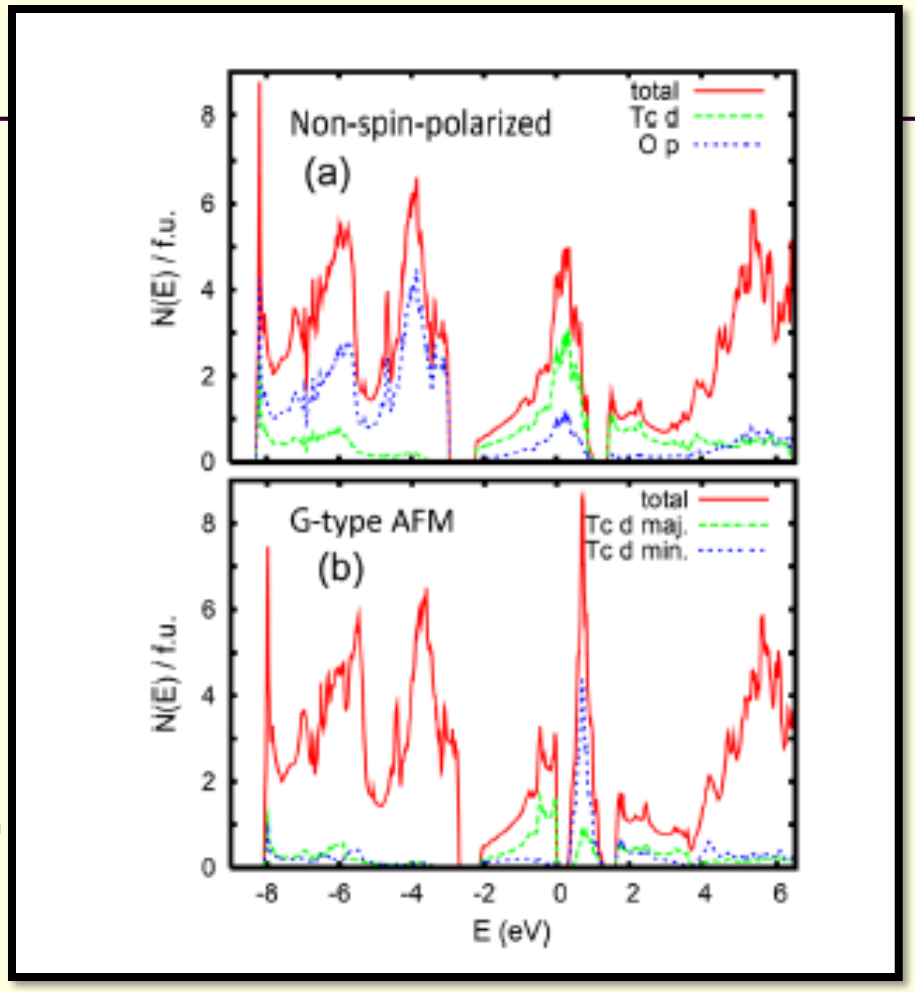

Should a Stoner mechanism lead to a magnetic instability?

N(Ef) = 4.3 ; Not all of it is on Tc!!

Constrained moment calculations in the FM ground state don't find *a magnetic minimum*

Rodriguez et al., PRL 106, 067201 (2011)

$CaTcO_3$

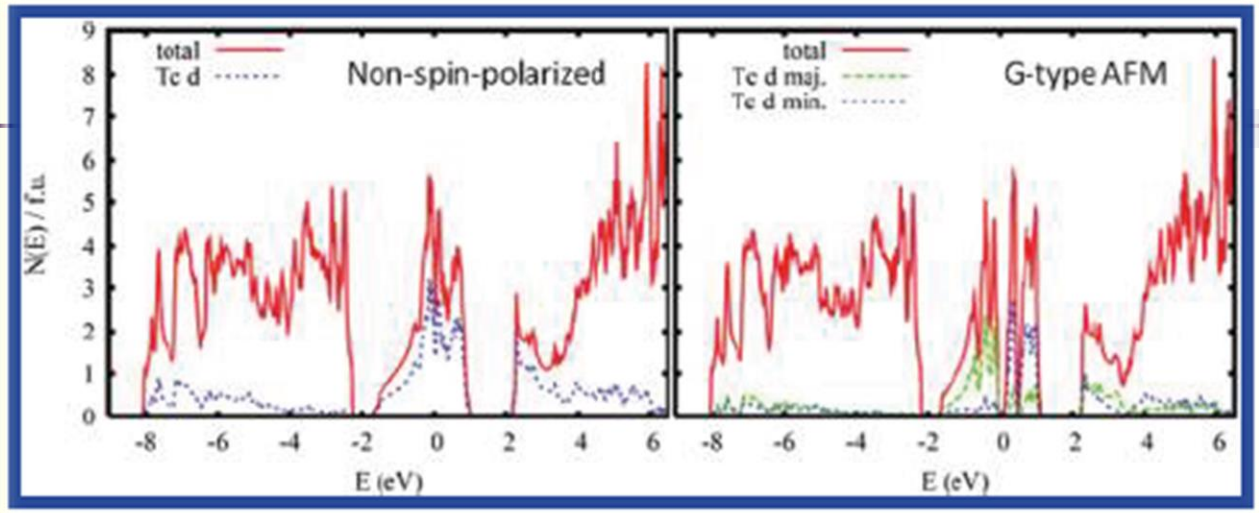

Energies of different magnetic configurations relative to the nonmagnetic state

FM	-0.003 eV	(0.5 μB)
A-AFM	-0.005 eV	(0.4 μB)
C-AFM	-0.040 eV	
G-AFM	-0.078 eV	(1.3 μB)

Avdeev et al., JACS 133, 1654 (2011).

TABLE II. Compilation of measured and calculated magnetic moment m, exchange coupling constants T_N and relative stability of the different magnetic phases considered [$\Delta E_{GC} = E(\mathrm{AFM}-C) - E(\mathrm{AFM}-G)$, $\Delta E_{GA} = E(\mathrm{AFM}-A) - E(\mathrm{AFM}-G)$, and $\Delta E_{GF} = E(\mathrm{FM}) - E(\mathrm{AFM}-G)$] for $R\mathrm{TcO_3}$ (R = Ca, Sr, and Ba). Experimental data (m, taken at 4 K, and T_N) are available only for $\mathrm{CaTcO_3}$[5] and $\mathrm{SrTcO_3}$.[6]

	$\mathrm{CaTcO_3}$		$\mathrm{SrTcO_3}$		$\mathrm{BaTcO_3}$
	Expt.	Calc.	Expt.	Calc.	Calc.
m (μ_B)	~2.0	2.10	2.13	2.04	2.04
ΔE_{CG} (meV/f.u.)	–	81	–	121	139
ΔE_{AG} (meV/f.u.)	–	191	–	289	299
ΔE_{FG} (meV/f.u.)	–	313	–	449	439
J_1 (meV)	–	−26.2	–	−35.3	−34.0
J_2 (meV)	–	−1.3	–	−0.7	0.1
T_N (K)	800	750	1020	1135	1218

C. Franchini et al, PRB 83 220402(R)(2011).

What are the relevant energetics?

Robust G-AFM state always found in the calculations with the other magnetic states struggling to exist.

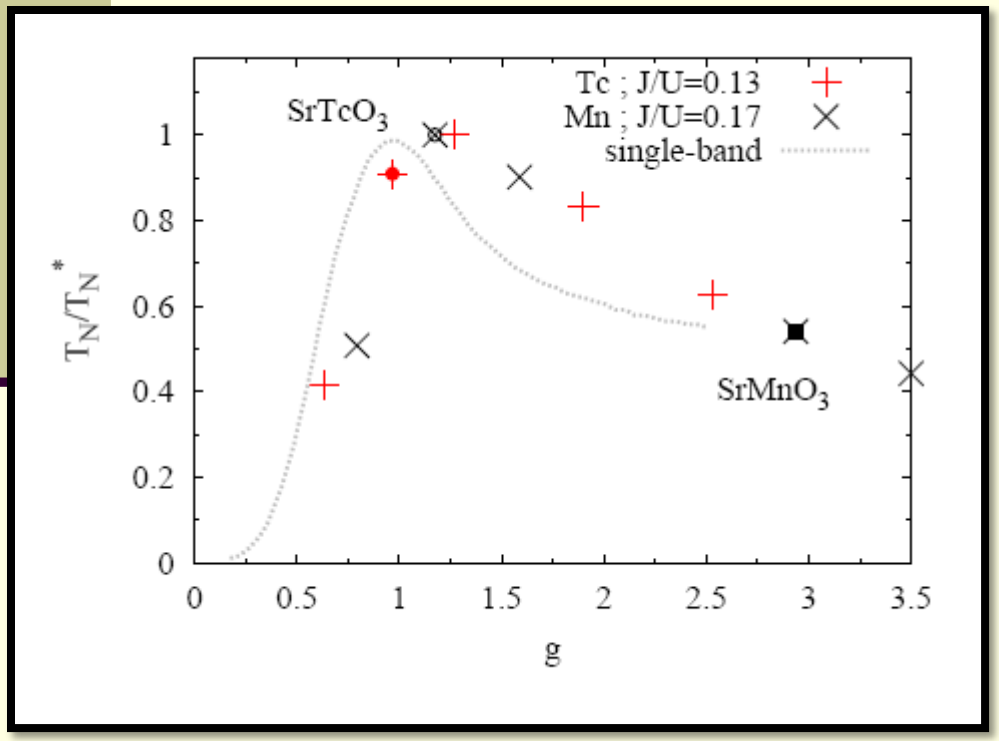

$SrTcO_3$ sits at the boundary between the itinerant to localized regime and hence has such a high transition temperature.

J. Mravlje, M. Aichhorn, and A. Georges, Phys. Rev. Lett. 108, 197202 (2012).

High magnetic ordering temperatures found in ab-initio calculations with moments comparable with experiment.

But why do we have such high magnetic ordering temperatures?

Stabilization energy in meV/f.u. wrt nonmag (GGA+U)

U (eV)	Ferro	AAFM	CAFM	GAFM
0	Nonmag	Nonmag	-46	-168
2	-432	-568	-662	-745
3	-925	-1029	-1100	-1164

So our calculations could reproduce earlier ab-initio calculations

Stability is larger for more antiferromagnetic neighbours

A multiband Hubbard-like Hamiltonian

$$H = \sum_{i,l,\sigma} \epsilon_p p^{\dagger}_{il\sigma} p_{il\sigma} + \sum_{i,l,\sigma} \epsilon^{l}_{d} d^{\dagger}_{il\sigma} d_{il\sigma}$$

$$+ \sum_{i,j,l_1,l_2,\sigma} t^{l_1 l_2}_{ij,pp} p^{\dagger}_{il_1\sigma} p_{jl_2\sigma} + \sum_{i,j,l_1,l_2,\sigma} t^{l_1 l_2}_{ij,pd} d^{\dagger}_{il_1\sigma} p_{jl_2\sigma}$$

$$+ \text{h.c} \quad + \sum_{\alpha\beta\gamma\delta,\sigma_1\sigma_2\sigma_3\sigma_4} U^{\alpha\beta\gamma\delta}_{dd} d^{\dagger}_{\alpha\sigma_1} d^{\dagger}_{\beta\sigma_2} d_{\gamma\sigma_3} d_{\delta\sigma_4}$$

S. Middey et al., Phys. Rev. B **86**, 104406 (2012)

Determining parameters for the one electron part of the Hamiltonian

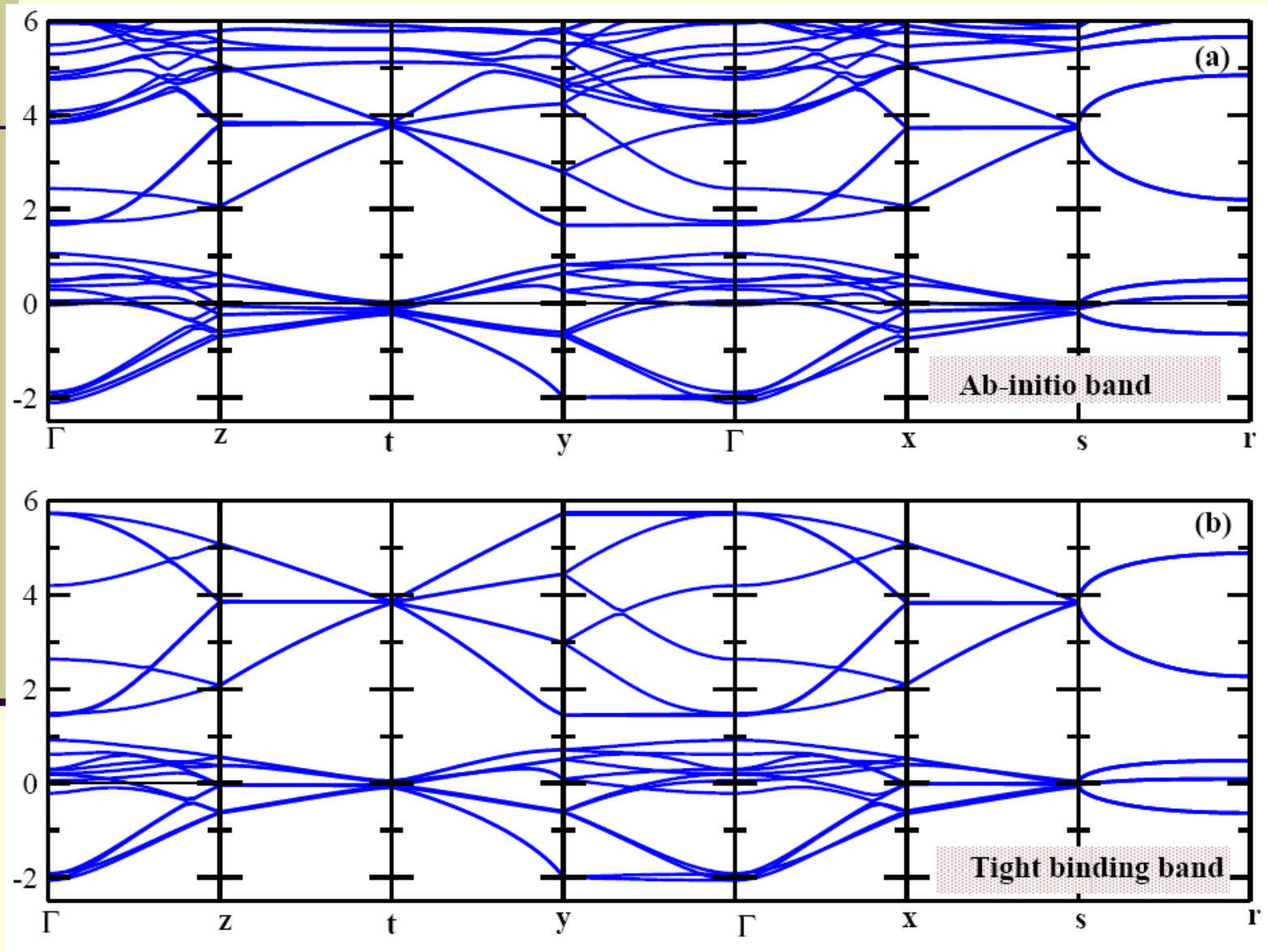

S. Middey et al., Phys. Rev. B **86**, 104406 (2012)

$pp\sigma$ =0.6 eV, $pp\pi$ =-0.10, $sd\sigma$ = -3.4 eV,
$pd\sigma$ = -3.3 eV, $pd\pi$ = 1.5 eV

Note that $pd\pi$ was found to be 1.2 eV for $SrMnO_3$ from a similar analysis

Varied U, Delta, J_h

S. Middey et al., Phys. Rev. B **86**, 104406 (2012)

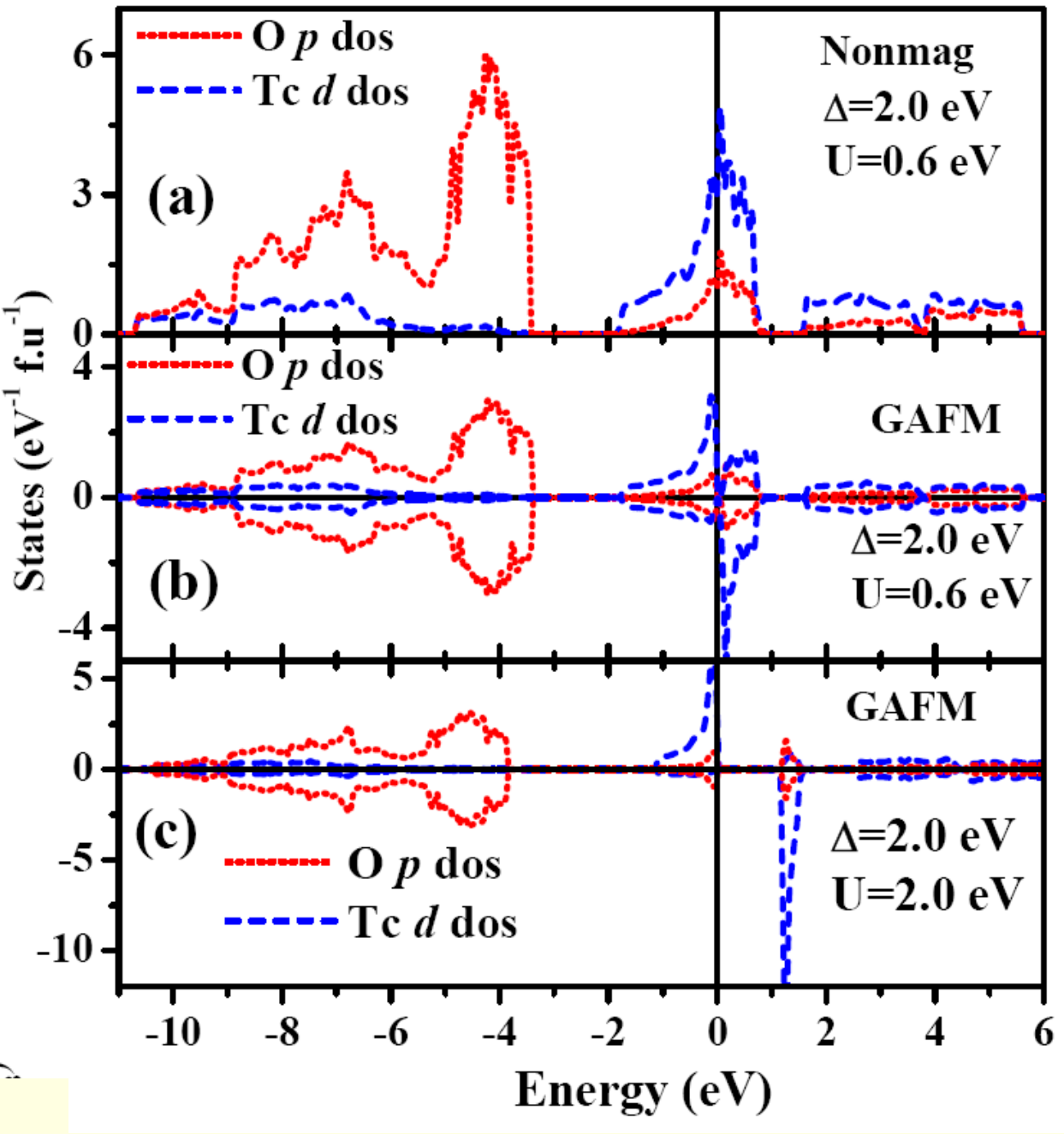

J_h is taken to be 0.1 eV, and still we see magnetic order !

S. Middey et al., Phys. Rev. B **86**, 104406 (2012)

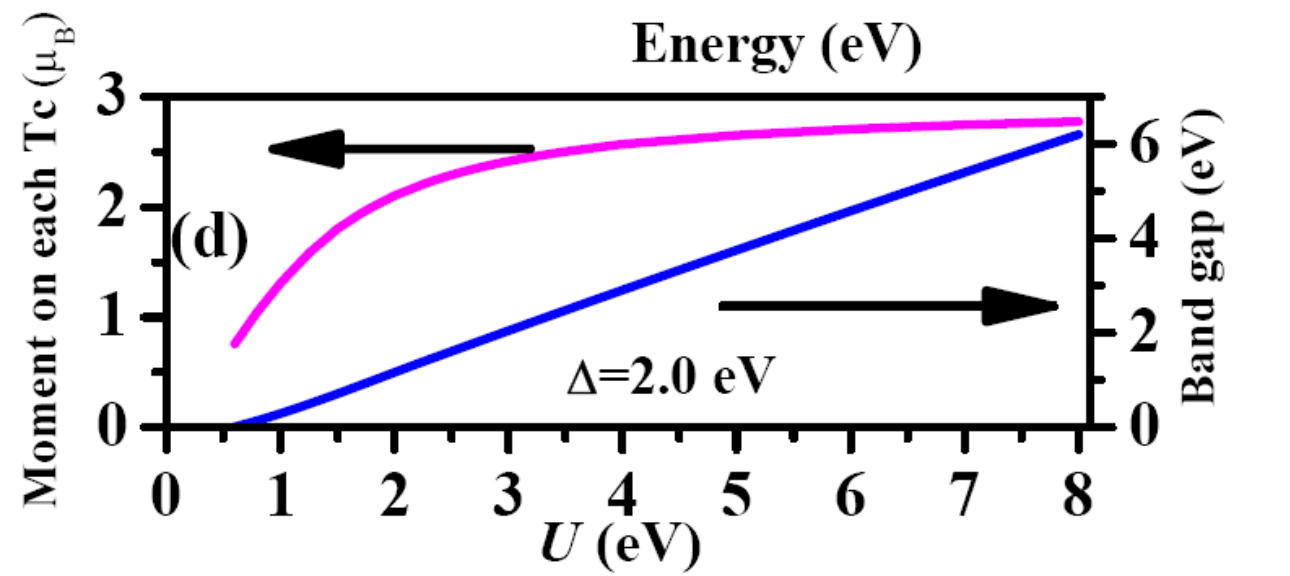

Note the small moment at small U for a d^3 system

S. Middey et al., Phys. Rev. B **86**, 104406 (2012)

Comparison between $SrMnO_3$ and $SrTcO_3$

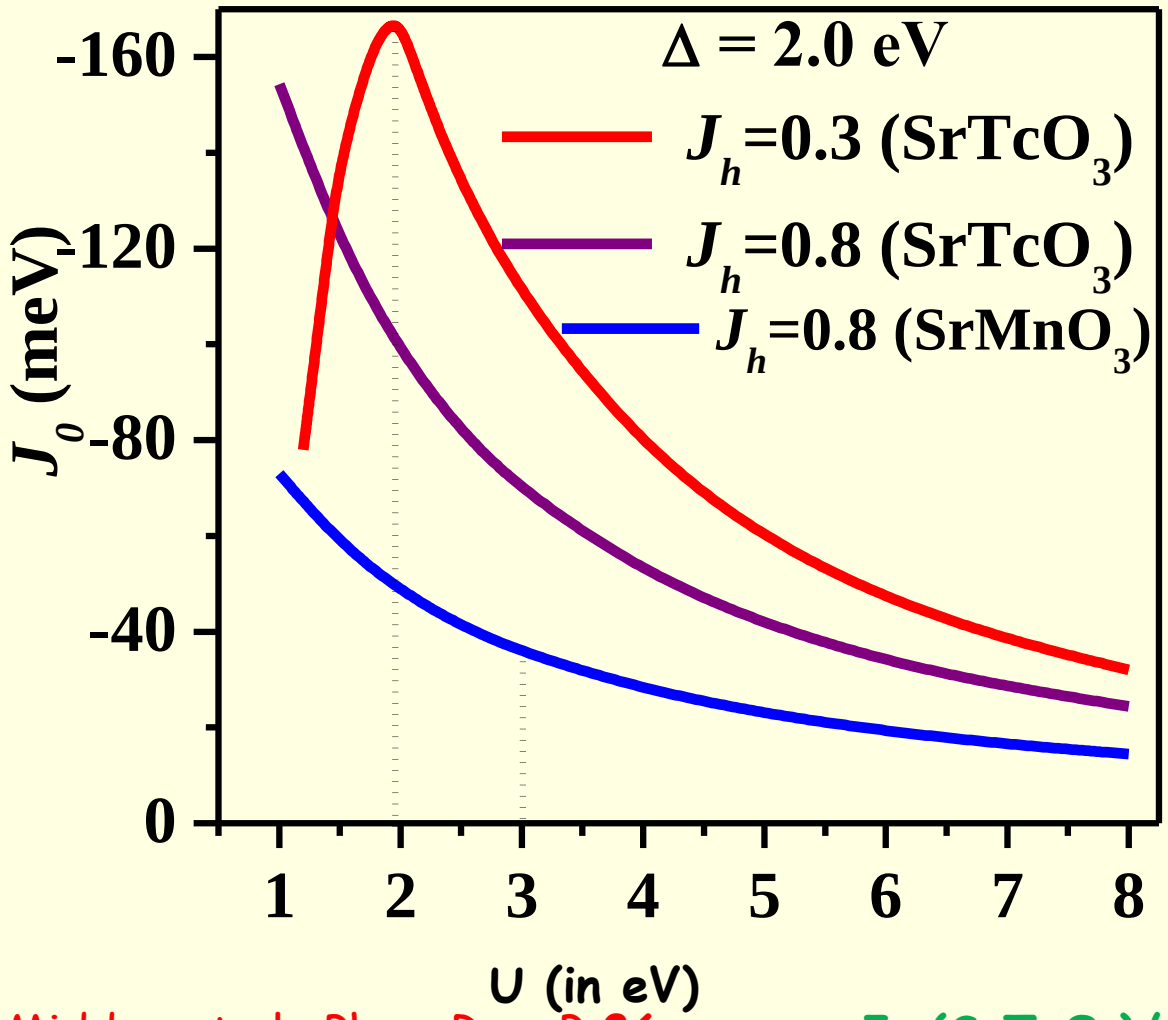

S. Middey et al., Phys. Rev. B **86**, 104406 (2012)

J_0 ($SrTcO_3$)/J_0($SrMnO_3$) = 4.4 same as experimentally observed T_N

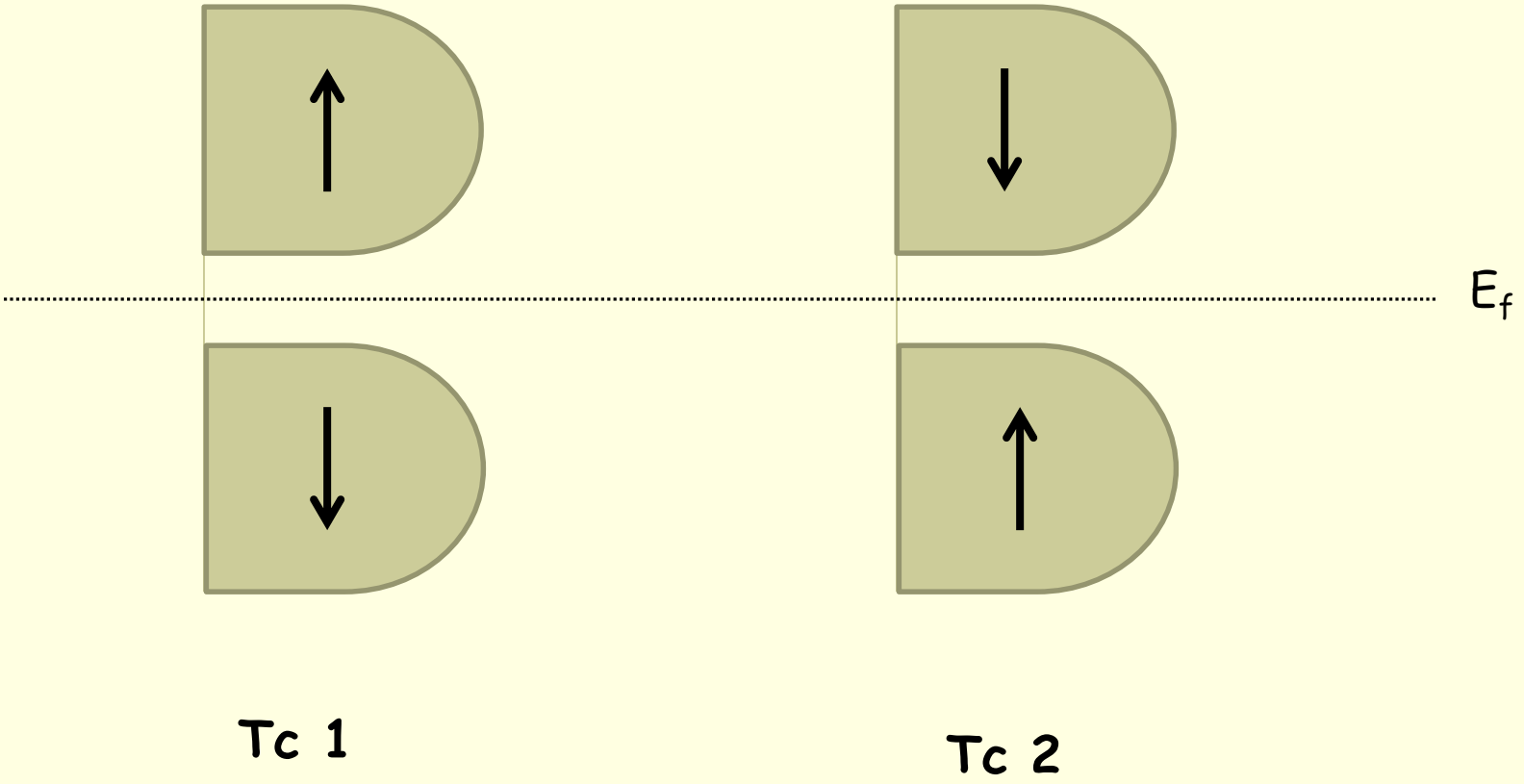
E_f
Tc 1
Tc 2

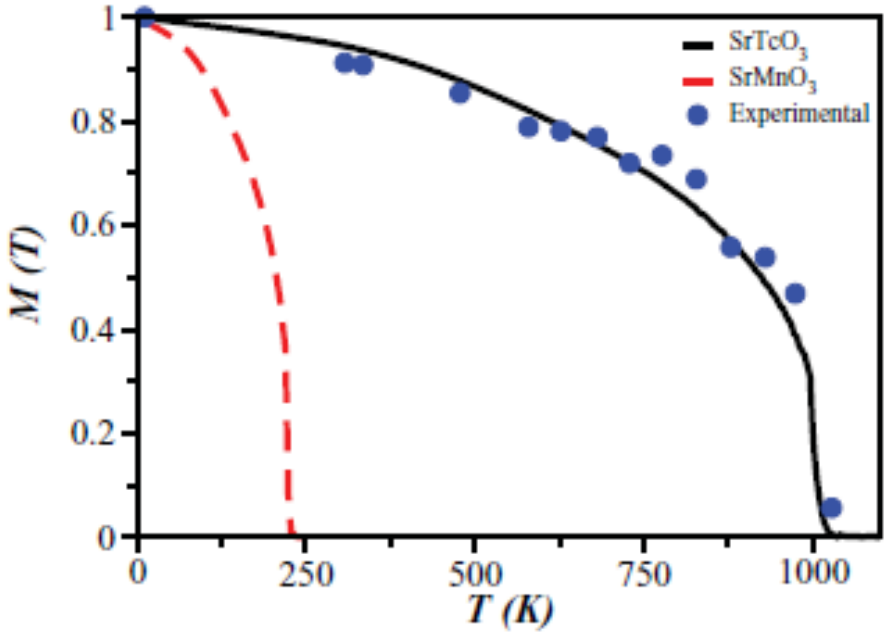

FIG. 5. (Color online) The variation of the magnetic moment as a function of temperature (T) for $SrTcO_3$ and $SrMnO_3$ calculated within a Heisenberg model with nearest neighbor (J_1) and next-nearest-neighbor (J_2) exchange interactions. The experimental variations (solid circle) for the saturation magnetic moment from Ref. 27 are provided for $SrTcO_3$.

S. Middey et al., Phys. Rev. B **86**, 104406 (2012)

Are there other examples among other d^3 compounds?

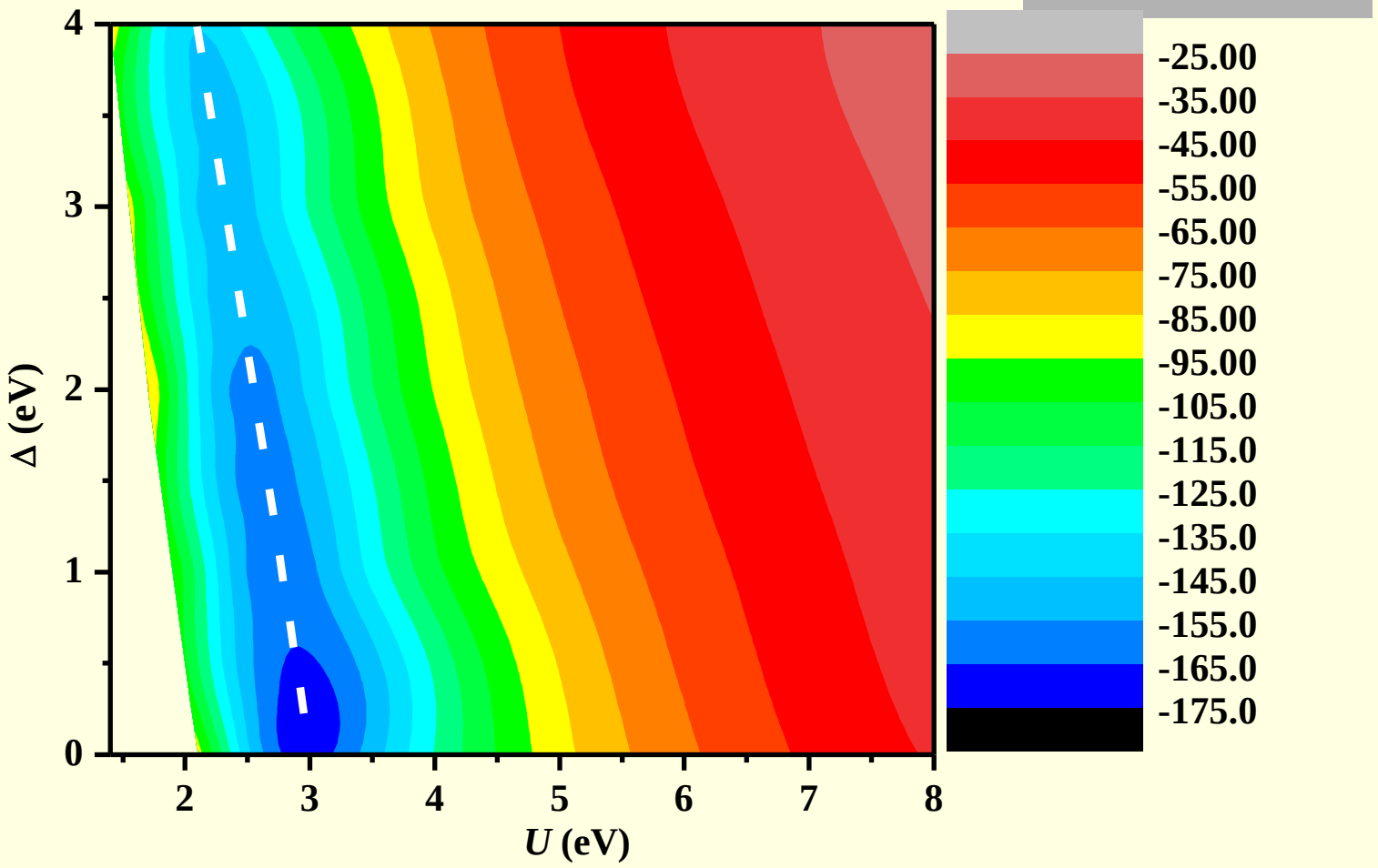
4
3
2
1
0
Δ (eV)
2
3
4
5
6
7
8
U (eV)
-25.00
-35.00
-45.00
-55.00
-65.00
-75.00
-85.00
-95.00
-105.0
-115.0
-125.0
-135.0
-145.0
-155.0
-165.0
-175.0

$NaOsO_3$ - first Slater insulator?

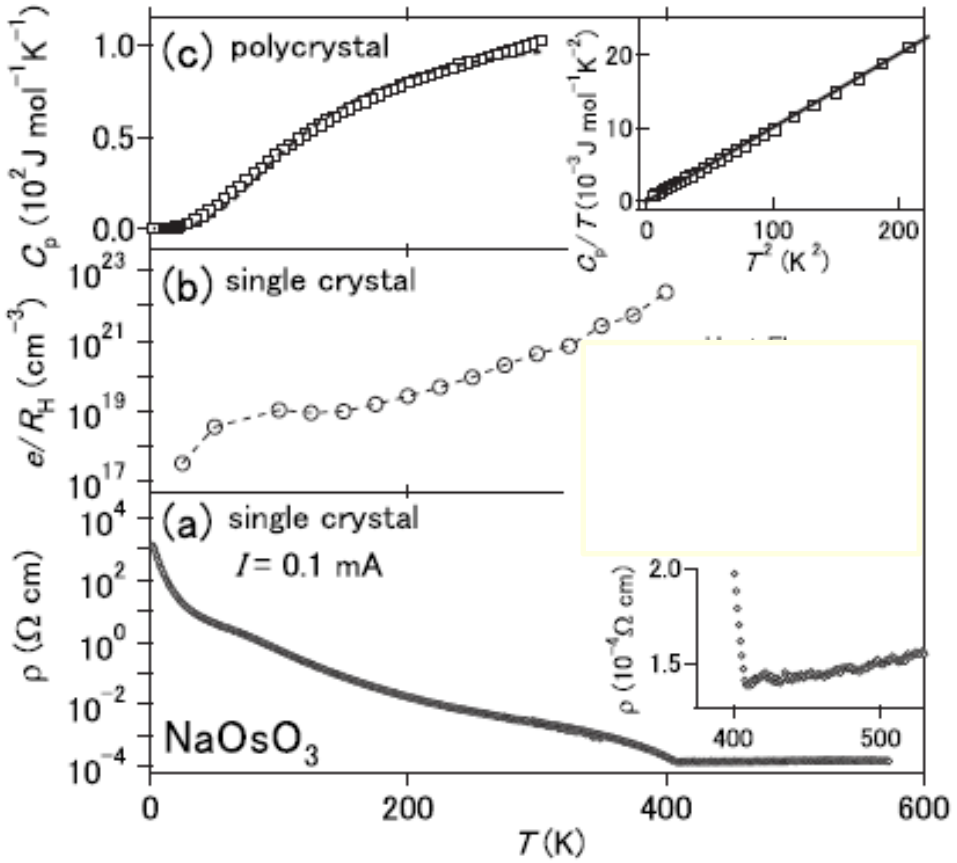

FIG. 2. T dependence of (a) ρ, (b) R_H, and (c) C_p of $NaOsO_3$. The inset shows an expansion of ρ vs T, DSC curves, and C_p/T vs T^2 (solid line is a fit to the data) at the low-temperature limit. The data were measured by a van der Pauw method on the assumption that the charge transport of the crystal is isotropic in nature.

A metal insulator transition below 410 K

Shi et al,
PRB **80**, 161104 (2009).

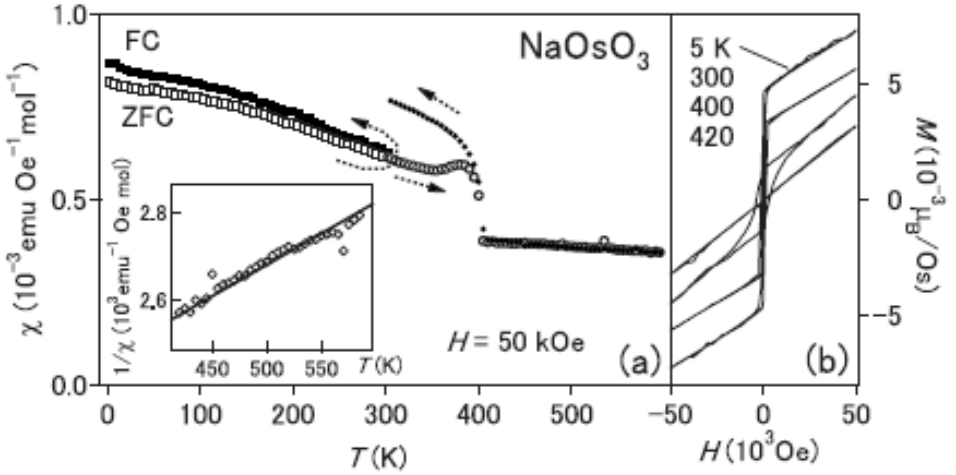

FIG. 3. (a) T dependence of χ of amount of single crystals of $NaOsO_3$, measured separately below (squares) and above (circles) 300 K. The inset shows an alternative plot of the data above 410 K. (b) Isothermal magnetization of $NaOsO_3$. The measurements were conducted on crystals randomly oriented in a sample holder.

Shi et al,
PRB **80**, 161104 (2009).

Transition from metallic, paramagnetic state to insulating, antiferromagnetic state at 410 K.

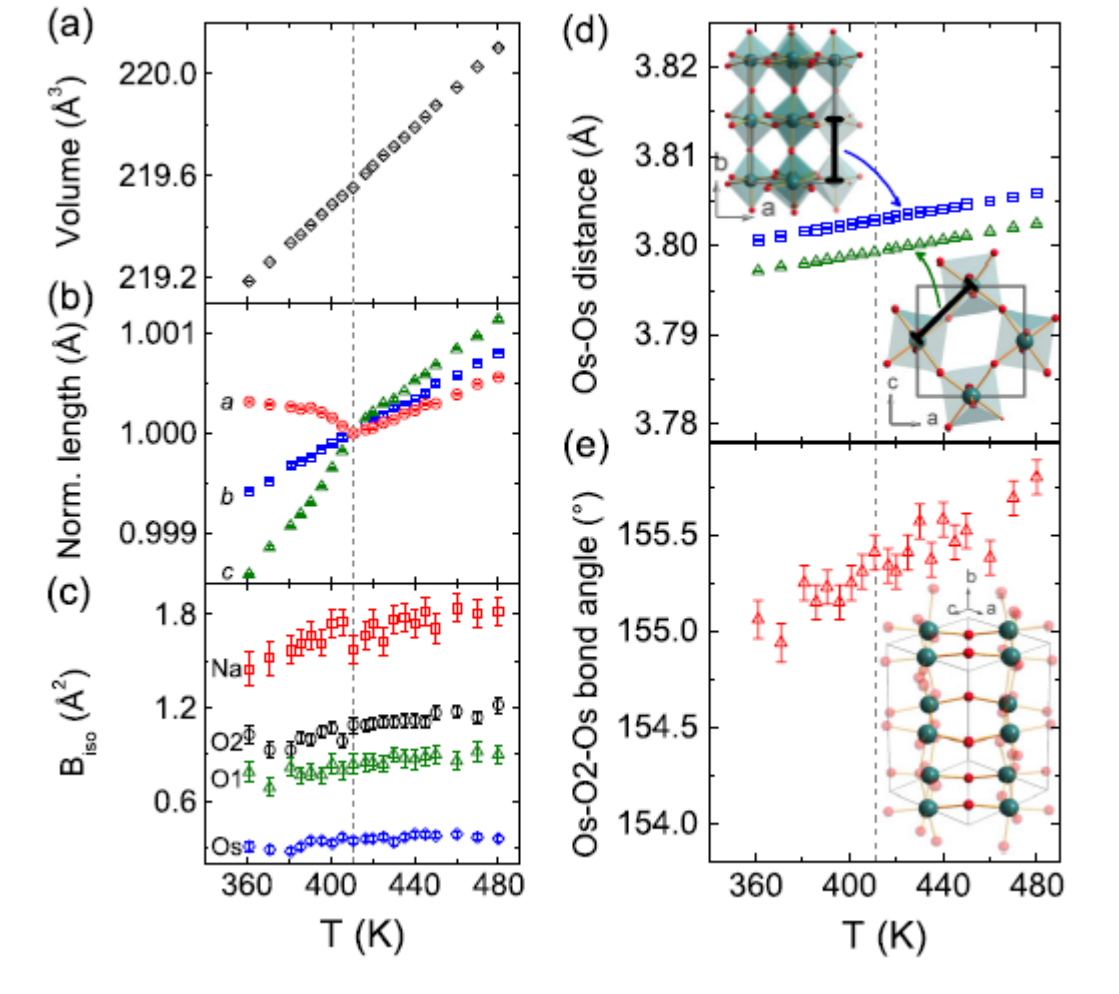

Calder et al., PRL 108 257209 (2012).

Stabilization energy in meV/f.u. wrt nonmag

U (eV)	Ferro	AAFM	CAFM	GAFM
0	Nonmag	Nonmag	nonmag	-20
1	-7	-11	-49	-127
3	-295	-415	-521	-587

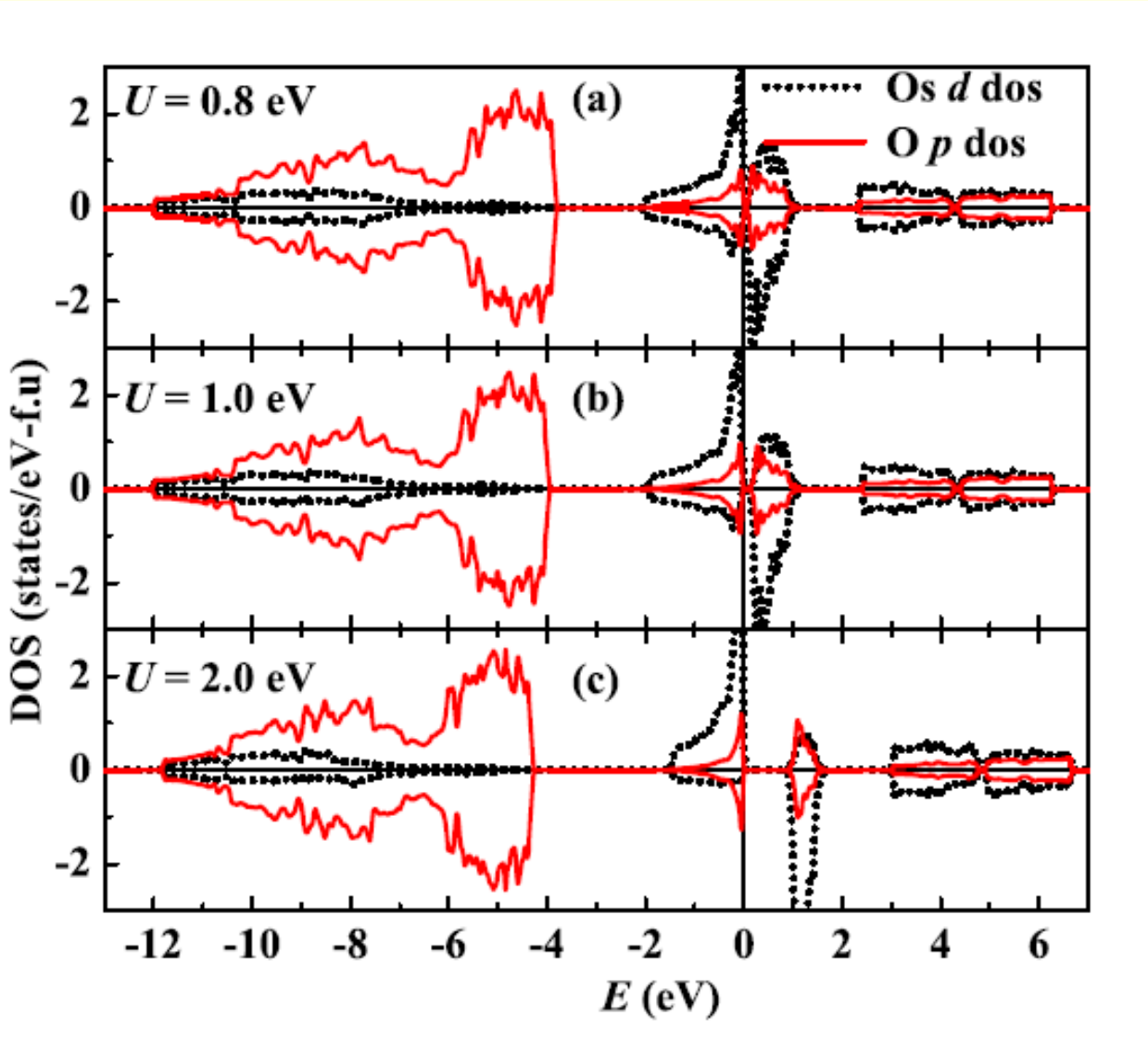

S. Middey et al., Phys. Rev. B **89**, 134416 (2014)

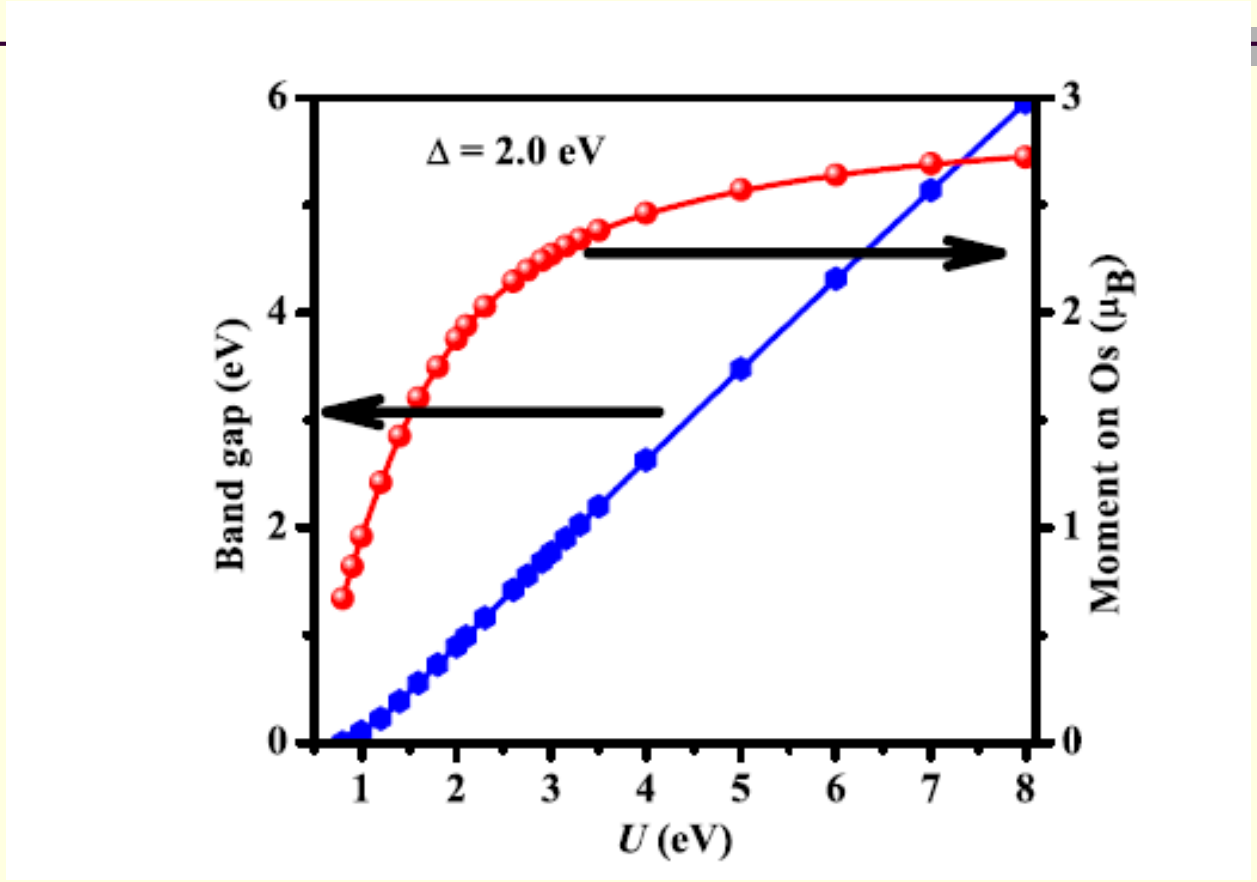

S. Middey et al., Phys. Rev. B **89**, 134416 (2014)

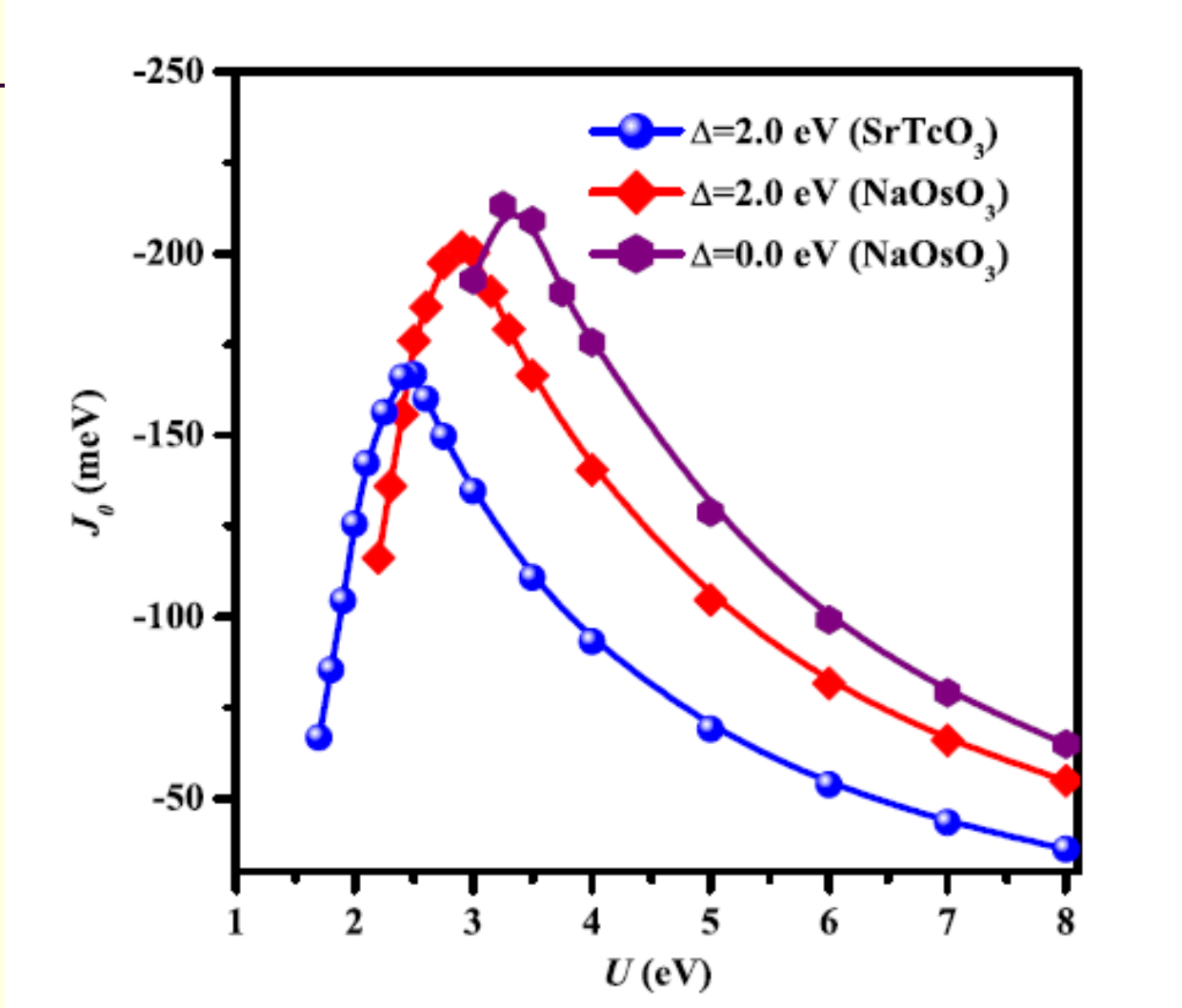

S. Middey et al., Phys. Rev. B **89**, 134416 (2014)

High magnetic ordering temperatures among the 4d and 5d transition metal oxides are shown to be a generic feature of the half-filled limit.

Why do we want antiferromagnetic metals?

An active component of antiferromagnetic spintronics*

Need antiferromagnetic metals for spin injectors, electrodes of magnetoresistance device

Ferromagnetism ⟺ Metallicity

Antiferromagnetism ⟺ Insulating state

*T. Jungwirth et al., Nature Nano 11, 231 (2016).

Single band Hubbard model results

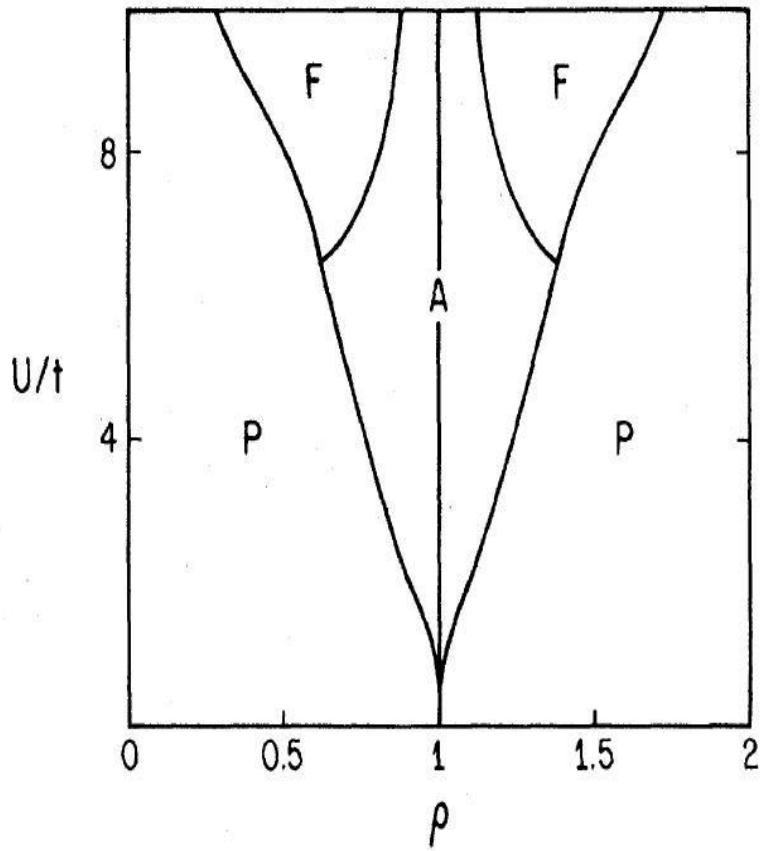

FIG. 3. Hartree-Fock phase diagram for the two-dimensional Hubbard model. *A*, *F*, and *P* denote antiferromagnetic, ferromagnetic, and paramagnetic ground states, respectively.

Suggests a prescription

Hirsch *et. al.* , Phys. Rev. B 31, 4403 (1985).

Where is the antiferromagnetic metallic phase?

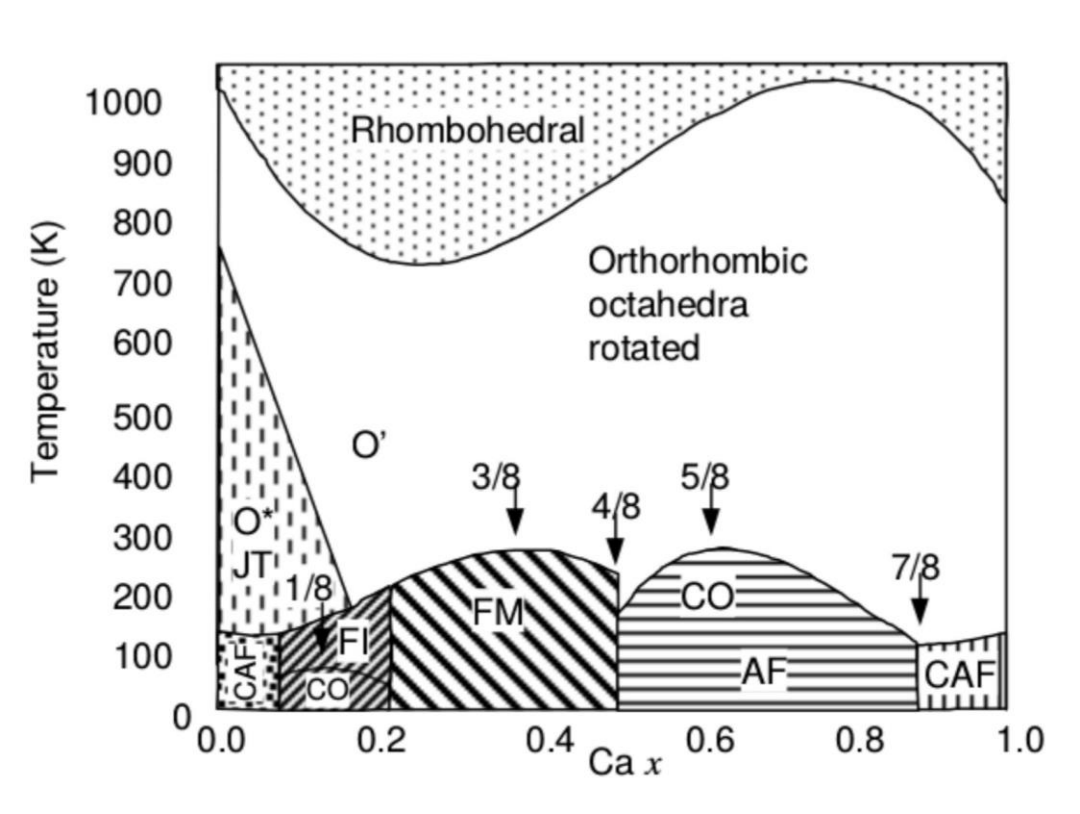

Uehara *et. al.* Chatterji T (ed) 2004 Colossal Magnetoresistance Manganites (Dordrecht: Kluwer Academic)

The case of 5*d* orbitals : 25% electron doping

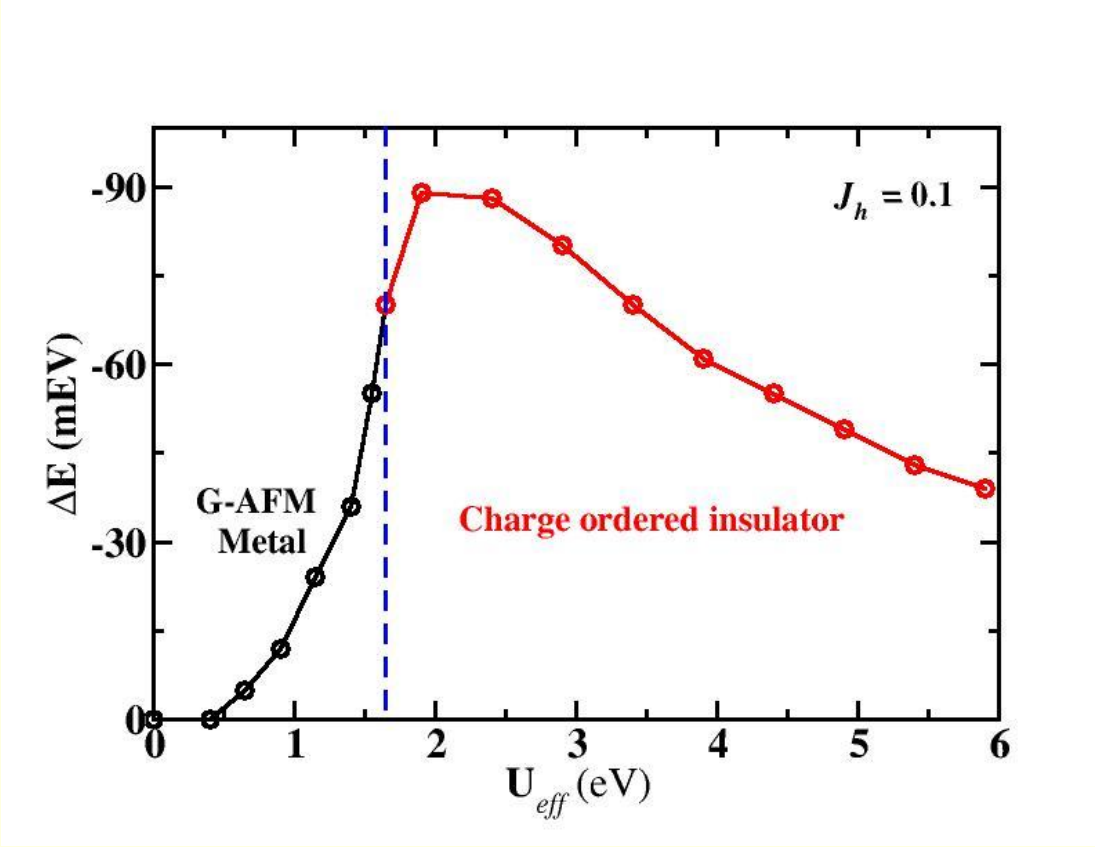

No ferromagnetism at high U.

An antiferromagnetic metallic phase is stabilized.

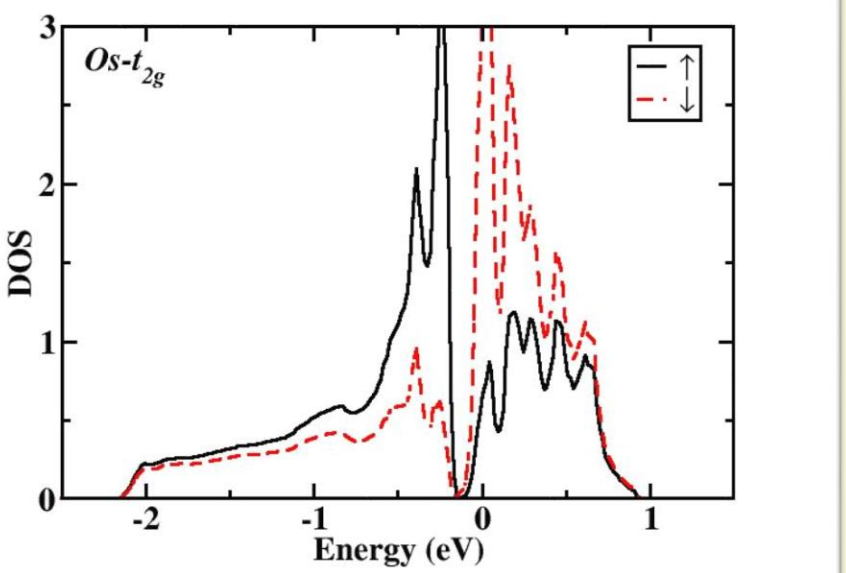
Os-t_{2g}
DOS
Energy (eV)
3
2
1
0
-2
-1
0
1

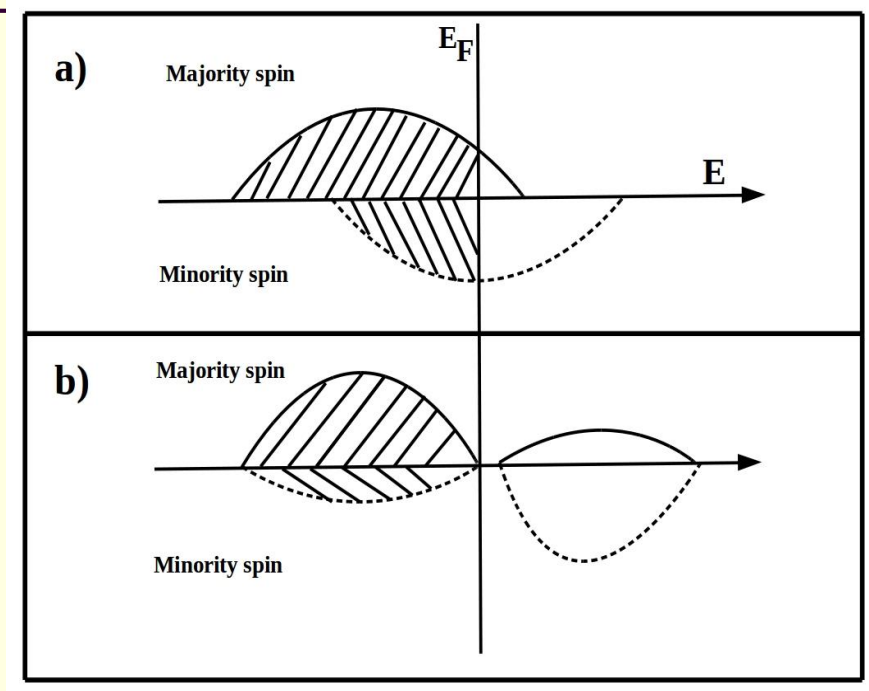
a)
Majority spin
E_F
E
Minority spin
b)
Majority spin
Minority spin

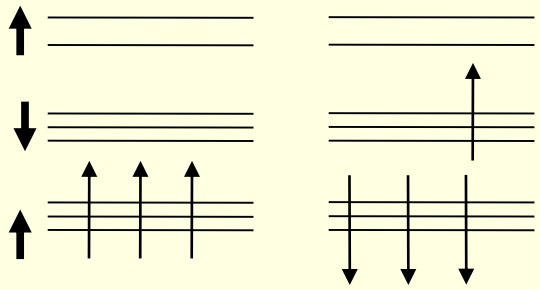

U= 1 eV

For a 5d transition metal oxide

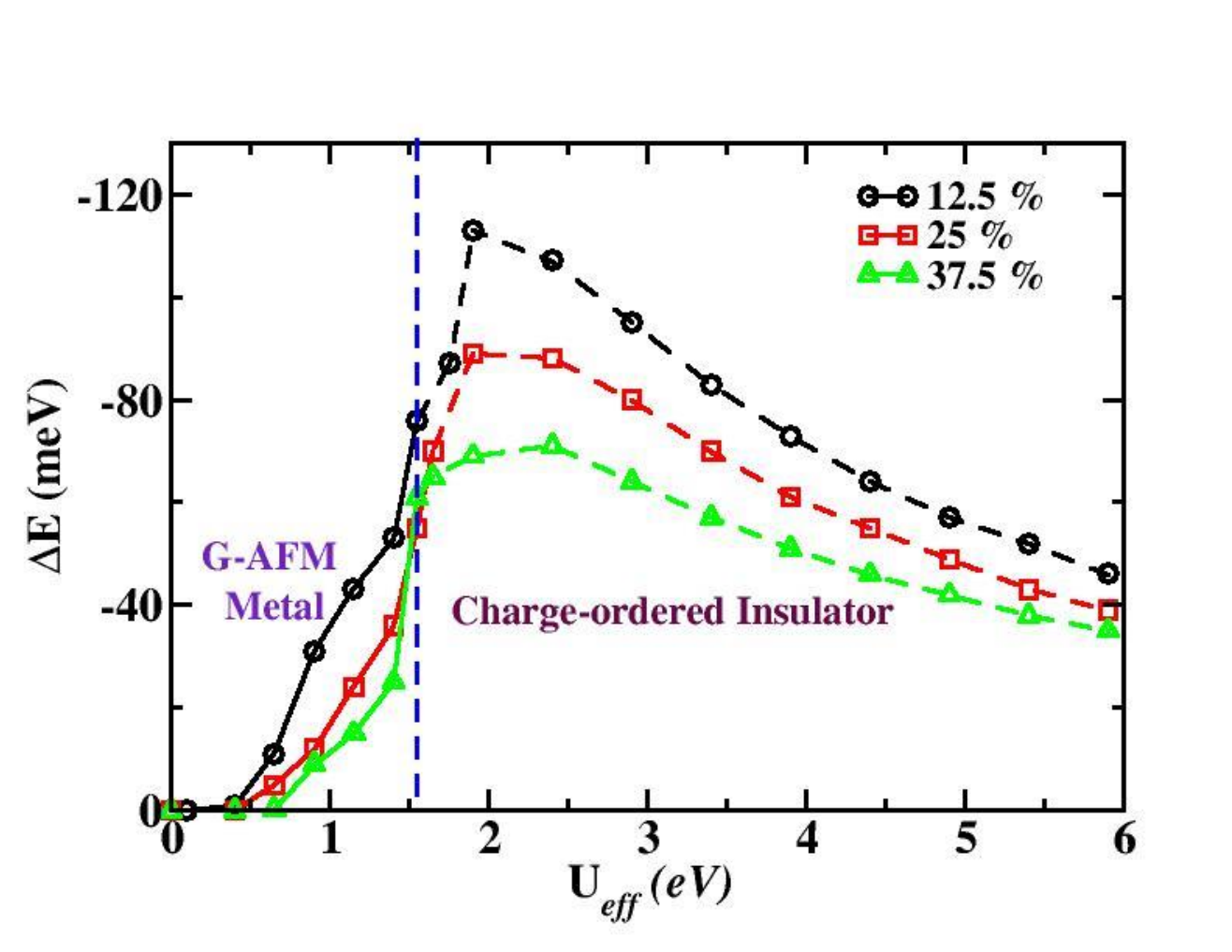

For a 3d transition metal oxide : 25% electron doping

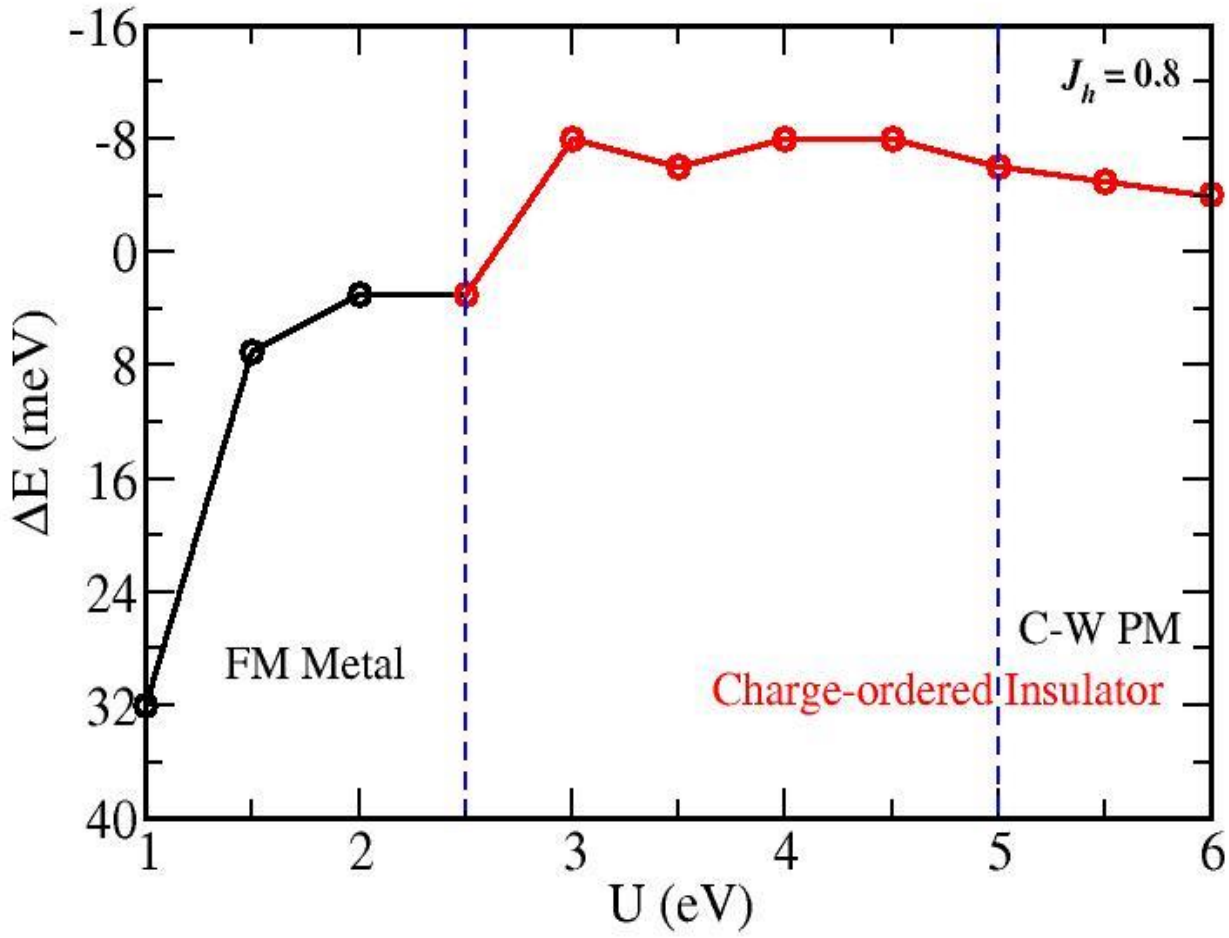

No Antiferromagnetic metallic phase

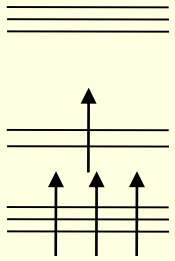

So, the Hund's intra atomic exchange interaction is found to play a role in determining the nature of magnetism in the doped transition metal oxides.

Role of orbital degeneracy

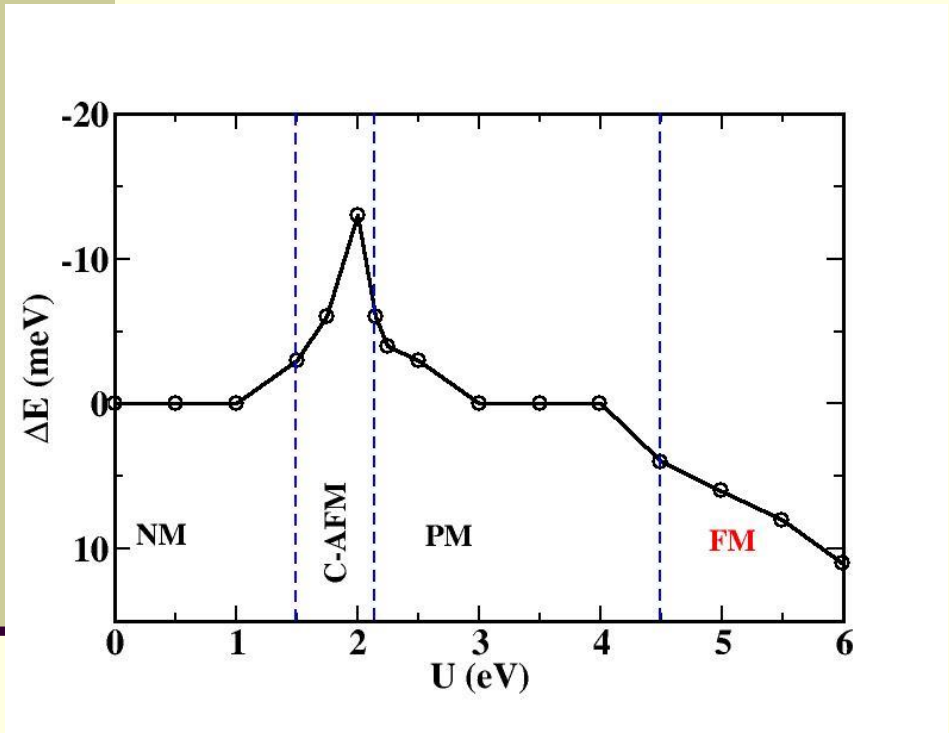

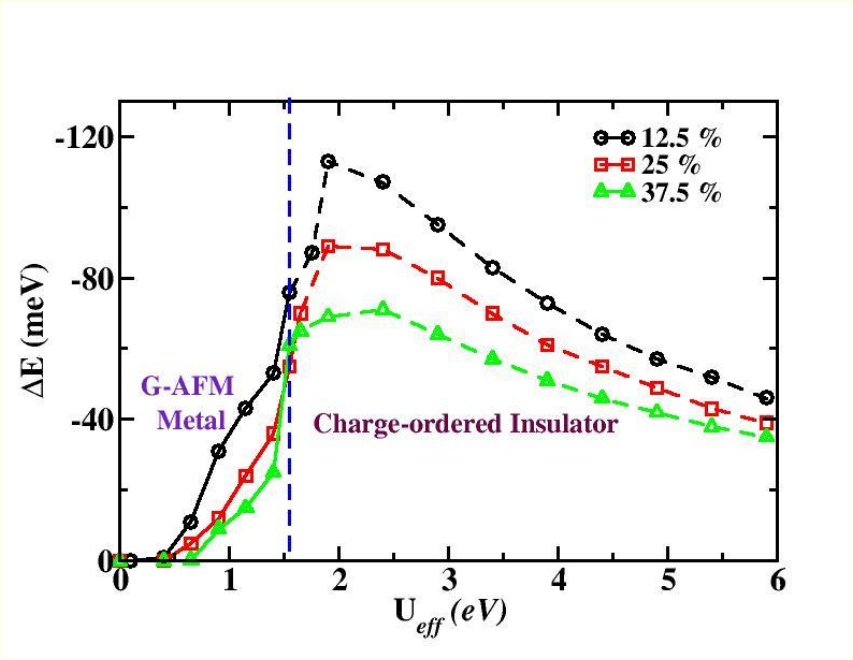

Hole Doped Case

5d oxide case :

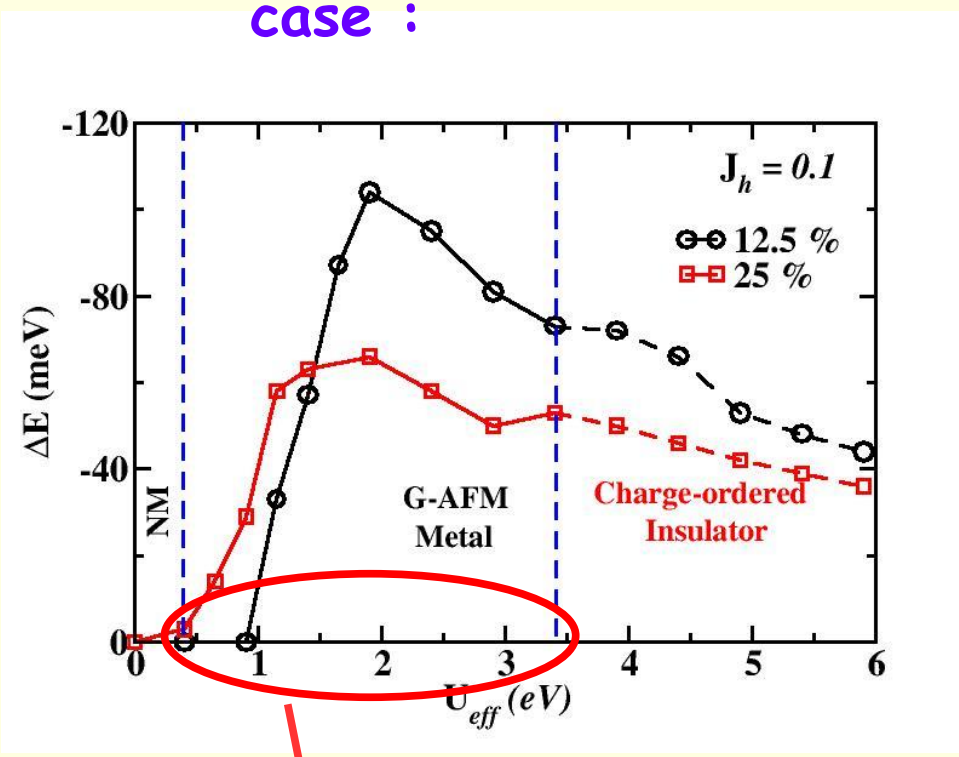

AFM-metallic phase is stabilized in a wider U range when compared to electron doping.

Hole Doped Case

3d oxide case :

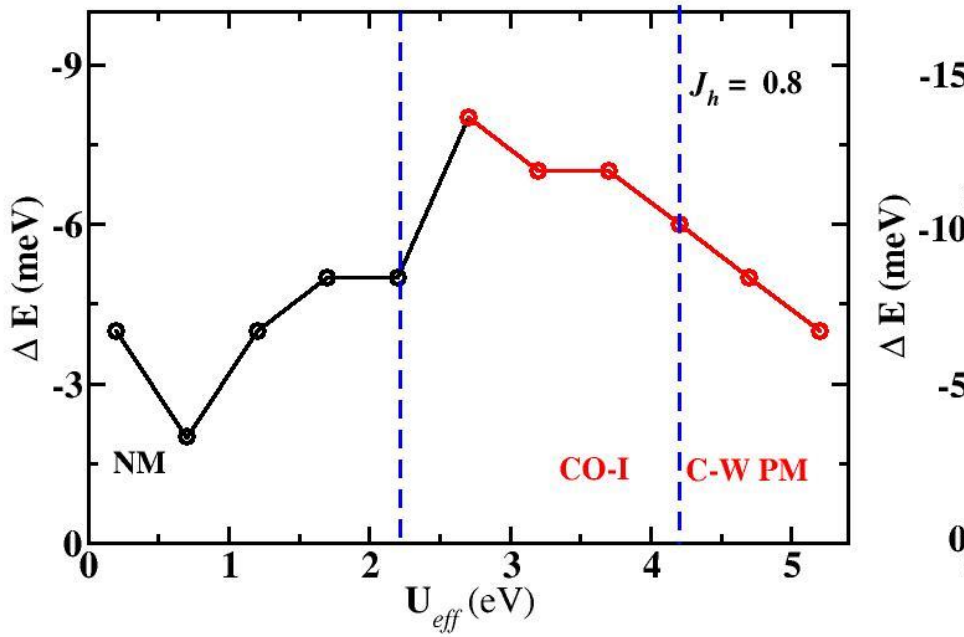

12.5 % doping

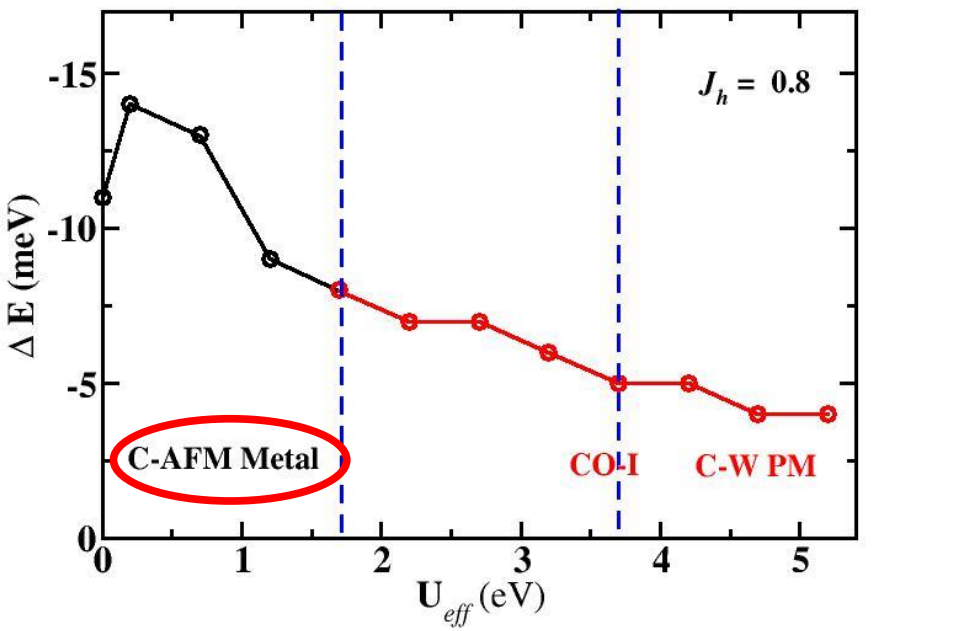

25 % doping

Electron-Hole Asymmetry

3d oxide case :

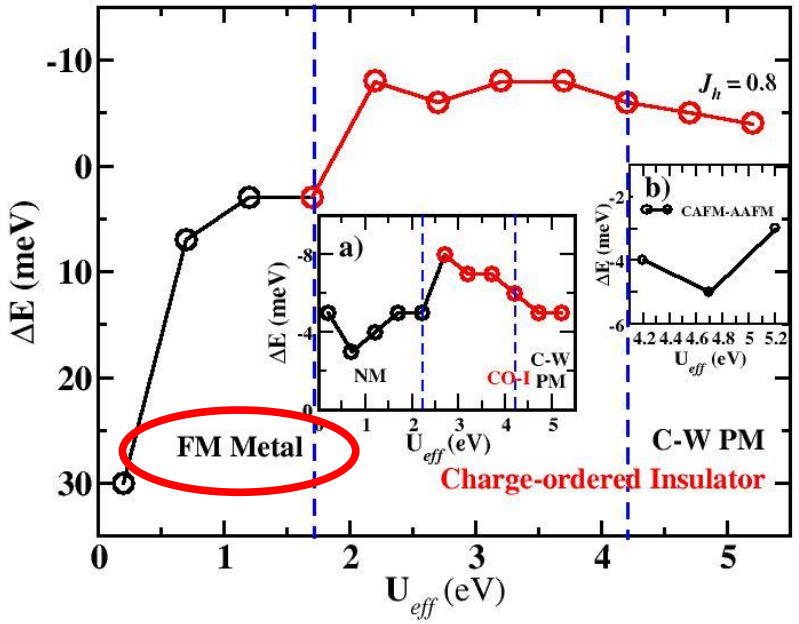

25 % electron doping

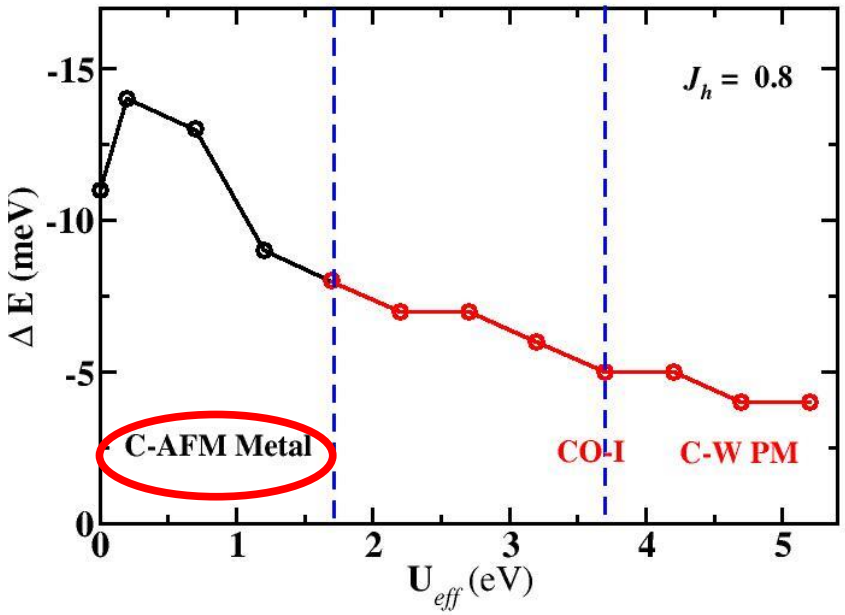

25 % hole doping

Srimanta Middey

Shishir Kumar Pandey

In collaboration with D.D. Sarma (IISc Bangalore)

S. Middey, A.K. Nandy, S.K. Pandey, P. Mahadevan and D.D. Sarma, PRB 86, 104406 (2012);
S. Middey, S. Debnath, P.Mahadevan and D.D. Sarma, PRB 89, 134416 (2014);
S.K. Pandey, P. Mahadevan and D.D. Sarma, EPL 117, 57003 (2017).

Funding acknowledged from
Department ofScience and Technology, India
Department of Atomic Energy, India

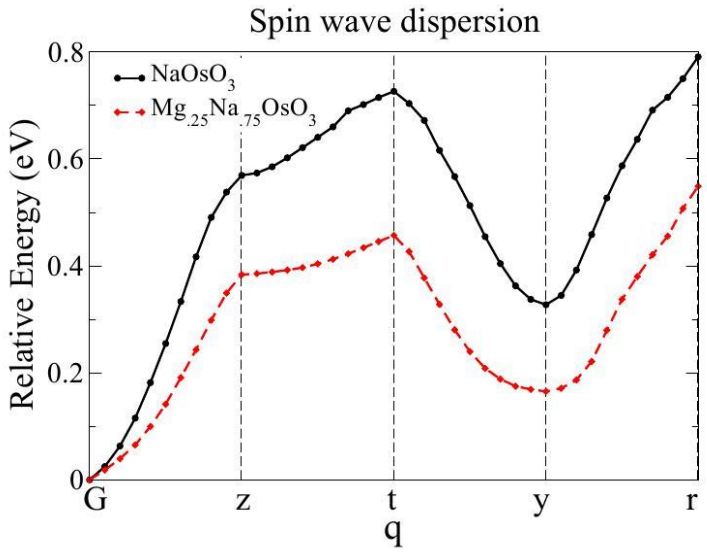

FIG. 8. (Color online) Spin wave dispersion along different symmetry directions for $NaOsO_3$ and 25% Mg doped case. The zero of energy corresponds to energy of G-AFM state for both cases.

Middey *et. al.* PRB 89, 134416 (2014)

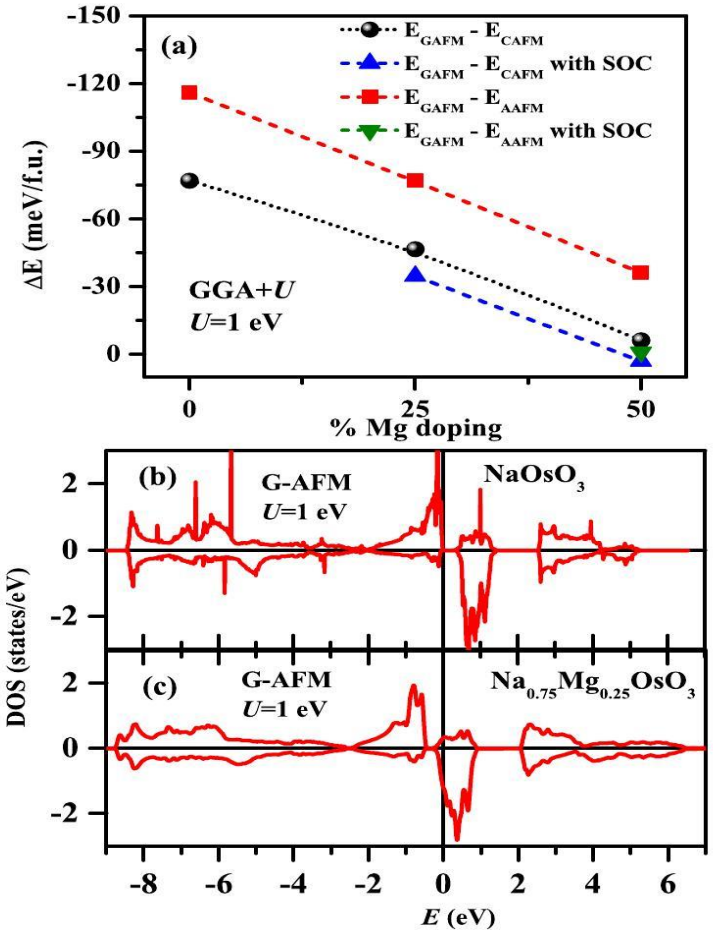

FIG. 5. (Color online) (a) Variation of magnetic stabilization energy of G-AFM configuration with Mg doping ($U = 1$ eV) from GGA + U calculations. Up (top) and down spin (bottom) Os d projected partial density of states for (b) $NaOsO_3$ and (c) $Na_{0.75}Mg_{0.25}OsO_3$ at $U = 1$ eV in the G-AFM configuration.